Electronic Supplementary Information

Atropisomer-based Construction of Macrocyclic Hosts that Selectively Recognize Tryptophan from Standard Amino Acids

Fei Yang,[a,b] Caiping Liu,[c] Di Yin,[a] Yanqing Xu,[b] Mingyan Wu,[c] Wei Wei*[a]*

[a]Department of Chemistry, Capital Normal University, Beijing 100048, China.

*Email: wwei@cnu.edu.cn

[b]Laboratory of Cluster Science, Ministry of Education of China, Beijing Key Laboratory of Photoelectronic/Electrophotonic Conversion Materials, School of Chemistry and Chemical Engineering, Beijing Institute of Technology, Beijing 100081, China.

*Email: xyq@bit.edu.cn

[c]State Key Lab of Structure Chemistry, Fujian Institute of Research on the Structure of Mater, Chinese Academy of Sciences, Fuzhou, 350002, Fujian, China.

Table of Contents

1. Experimental Section

1.1 General Method.

All the reagents involved in this research were commercially available and used without further purification unless otherwise noted. Solvents were either employed as purchased or dried prior to use by standard laboratory procedures. ^{1}H and ^{13}C NMR spectra were recorded on a Bruker AVANCE III 600 spectrometer. All chemical shifts are reported in ppm with residual solvents or TMS (tetramethylsilane) as the internal standards. High-resolution electrospray-ionization mass spectrometry (ESI-MS) experiments were conducted on a Thermo Fisher Q Exactive mass spectrometer. UV-vis spectroscopy studies were performed on a Shimadzu UV-2550 spectrophotometer.

1.2 Synthetic Routes of TBox-1.

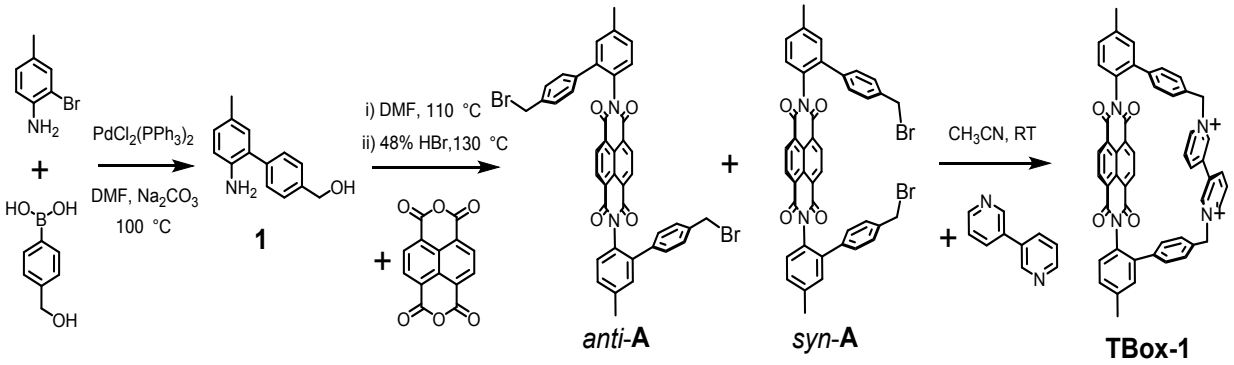

Synthesis of 1:

The solution of 2-bromo-4-methylaniline (7.00 g, 37.63 mmol) in DMF (115 mL) was degassed with nitrogen for 15 min followed by addition of Na_2CO_3 solution (75 mL, 2 M) under continuous flow of nitrogen. After 10 min, 4-(hydroxymethyl)phenylboronic acid (6.86 g, 45.16 mmol) and $PdCl_2(PPh_3)_2$ (1.81 g, 2.57 mmol) were added to the reaction mixture under a nitrogen atmosphere. The reaction mixture was stirred at 100 °C for 4 h. The solution was diluted with H_2O (25 mL), and then the product was extracted three times with ethyl acetate (EtOAc, 100 mL). The combined organic layer was dried over $MgSO_4$ and the solvent was removed in vacuo. The crude product was purified on a silica gel column using petroleum ether / ethyl acetate (3:1, v/v) as eluent to afford the product as yellow solid (6.40 g, 81%). **1**: ^{1}H

NMR (600 MHz, $CDCl_3$, 298 K): δ (ppm) = 7.435 (d, *J* = 8.4 Hz, 2H), 7.415 (d, *J* = 8.4 Hz, 2H), 6.966 (d, *J* = 7.8 Hz, 1H), 6.934 (s, 1H), 6.685 (d, *J* = 7.8 Hz, 1H), 4.714 (s, 2H), 2.270 (s, 3H). ^{13}C NMR (150 MHz, $CDCl_3$, 298 K): δ (ppm) = 140.85, 139.74, 138.95, 130.90, 129.22, 129.05, 127.99, 127.45, 127.42, 115.94 (C of biphenyl), 64.99 (C of methylene in phenylmethanol), 20.42 (C of methyl).

Synthesis of *syn*-**A**:

The mixture of **1** (5 g, 23.46 mmol) and 1,4,5,8-naphthalenetetracarboxylic dianhydride (2.51 g, 9.38 mmol) in DMF (100 mL) were stirred overnight at 110 °C under nitrogen protection. After cooling to room temperature, the mixture was poured into water (500 mL), and then the product was extracted three times with EtOAc (100 mL). The combined organic layer was dried over $MgSO_4$ and the solvent was removed in vacuo. The crude product was used for the next step without further purification. After the crude sample were stirred in HBr/H_2O (48% w/w, 50 mL) at 130 °C for 3h, the solution was diluted with H_2O (25 mL) and then extracted three times with EtOAc (100 mL). The combined organic layer was dried over $MgSO_4$ and the solvent was removed in vacuo to give a brown solid. The crude product was purified on a silica gel column using dichloromethane/petroleum ether (2:1, v/v) as eluent to give the higher R_f *anti*-**A** (2.868 g, 39%) and lower R_f *syn*- **A** (2.573 g, 35%), respectively.

Anti-**A**: ^1H NMR (600 MHz, $CDCl_3$, 298 K): δ (ppm) = 8.652 (s, 4H), 7.359 (d, *J* = 8.4 Hz, 2H), 7.310 (s, 2H), 7.244 (d, *J* = 7.8 Hz, 4H), 7.170 (d, *J* = 8.4 Hz, 4H), 7.163 (d, *J* = 7.8 Hz, 2H), 4.302 (s, 4H), 2.487 (s, 6H).

Syn-**A**: ^1H NMR (600 MHz, $CDCl_3$, 298 K): δ (ppm) = 8.652 (s, 4H), 7.357 (d, *J* = 7.8 Hz, 2H), 7.298 (s, 2H), 7.261 (d, *J* = 7.2 Hz, 4H), 7.199 (d, *J* = 7.2 Hz, 4H), 7.185 (d, *J* = 7.8 Hz, 2H), 4.340 (s, 4H), 2.483 (s, 6H); ^{13}C NMR (150 MHz, $CDCl_3$, 298 K): δ (ppm) = 162.94, 140.37, 139.67, 138.98 (C of naphthalene diimide), 136.83, 131.87, 131.22, 129.82, 129.74, 128.92, 128.57, 127.01, 126.57 (C of biphenyl), 33.16 (C of methylene in phenyl bromomethyl), 21.30 (C of methyl).

Synthesis of Tbox-1:

Syn-**A** (204 mg, 0.26 mmol) and 3,3'-bipyridine (3-bpy, 41 mg, 0.26 mmol) were stirred in dry CH_3CN at room temperature for 5 h under nitrogen protection. The yellow precipitate was collected by vacuum filtration and dissolved in H_2O. When a satd aqueous solution of NH_4PF_6 was added to the reaction mixture, the resulting precipitate was filtered off and then washed with deionized H_2O. The precipitate was dried to afford **TBox-1**·$2PF_6$ as a yellowish solid (198 mg, 71%). The final yield of **TBox-1**·$2PF_6$ reached 90% by the reaction with 5 equivalents of 3-bpy within 2 h. **TBox-1**·$2PF_6$: ^{1}H NMR (600 MHz, DMSO-d_6, 298 K): δ (ppm) = 9.586 (s, 2H), 9.398 (d, *J* = 6.6 Hz, 2H), 8.933 (d, *J* = 8.4 Hz, 2H), 8.561 (s, 4H), 8.403 (t, *J* = 7.2 Hz, 2H), 7.489 (d, *J* = 7.8 Hz, 2H), 7.396 (d, *J* = 7.8 Hz, 2H), 7.372 (d, *J* = 8.4 Hz, 4H), 7.310 (d, *J* = 8.4 Hz, 4H), 7.261 (s, 2H), 5.837 (s, 4H), 2.456 (s, 6H); ^{13}C NMR (150 MHz, DMSO-d_6, 298 K): δ (ppm) = 163.42, 145.65, 145.19, 144.55, 139.97, 139.57, 139.41, 134.38, 133.73, 132.12, 131.36, 130.45, 130.26, 129.95, 129.00, 128.87, 128.56, 126.97, 126.86 (C of aromatic rings), 63.70 (C of methylene), 21.15 (C of methyl). ESI-MS *m/z* calcd for [**TBox-1**]$^{2+}$: 390.1350, found: 390.1359 (100%); *m/z* calcd for [**TBox-1**+PF_6]$^+$: 925.2400, found: 925.2363 (100%).

TBox-1·$2PF_6$ was dissolved in CH_3CN followed by addition of tetrabutylammonium chloride, which yielded the corresponding water-soluble chloride **TBox-1**·2Cl as yellowish solids (95%). **TBox-1**·2Cl: ^{1}H NMR (600 MHz, D_2O : CD_3OD = 2 : 1, 298 K): δ (ppm) = 9.191 (s, 2H), 9.035 (d, *J* = 6.6 Hz, 2H), 8.724 (d, *J* = 8.4 Hz, 2H), 8.428 (s, 4H), 8.104 (t, *J* = 7.2 Hz, 2H), 7.214 (d, *J* = 8.4 Hz, 2H), 7.187 (d, *J* = 8.4 Hz, 4H), 7.187 (d, *J* = 8.4 Hz, 4H), 7.146 (s, 2H), 7.072 (d, *J* = 8.4 Hz, 2H), 5.689 (s, 4H), 2.253 (s, 6H). ESI-MS *m/z* calcd for [**TBox-1**]$^{2+}$: 390.1350, found: 390.1357 (100%); *m/z* calcd for [**TBox-1**+OH]$^+$: 797.2800, found: 797.2744 (100%); *m/z* calcd for [**TBox-1**+Cl]$^+$: 815.2400, found: 815.2406 (100%).

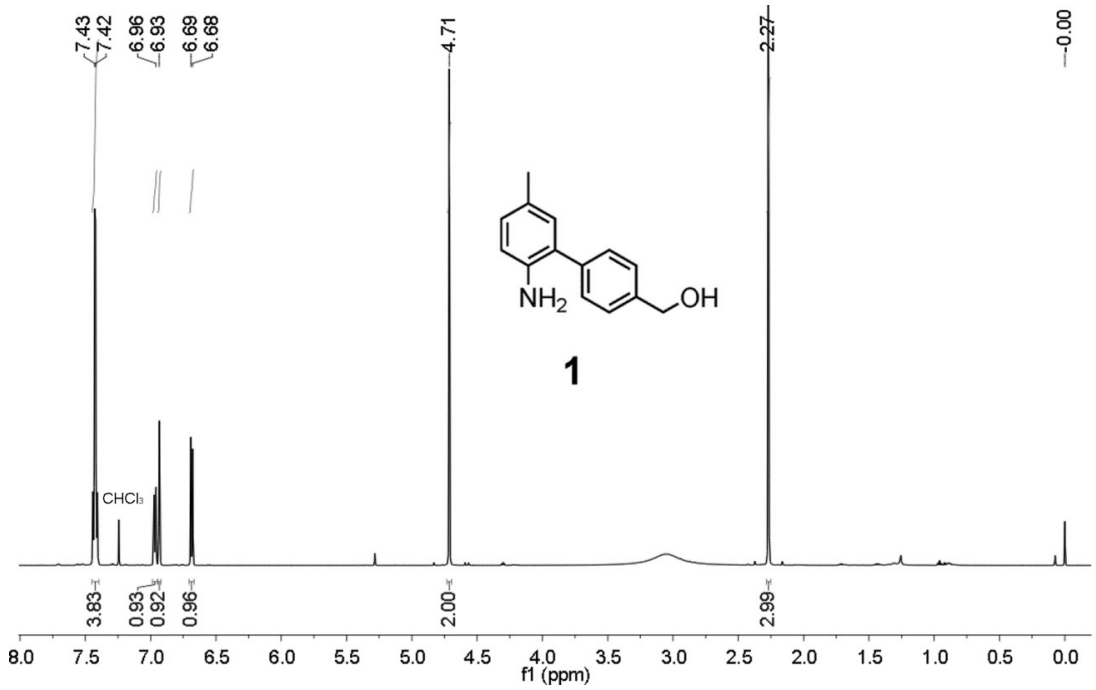

Fig. S1. ^{1}H NMR spectrum of **1** in $CDCl_3$.

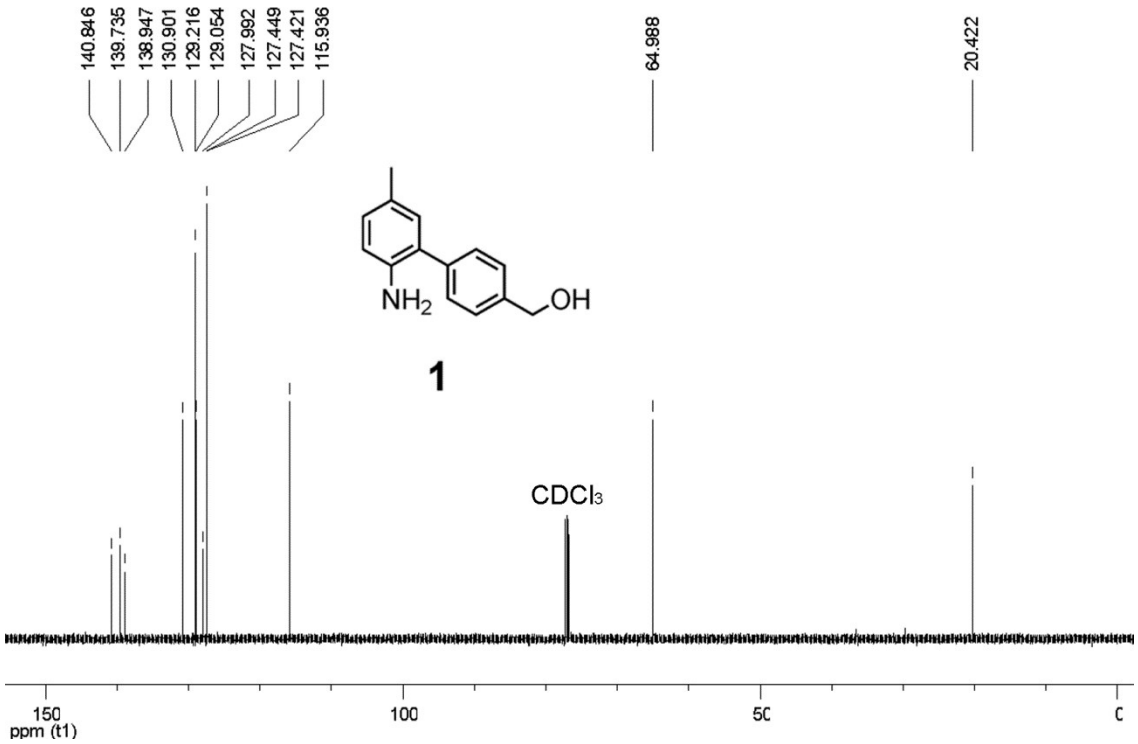

Fig. S2. ^{13}C NMR spectrum of **1** in $CDCl_3$.

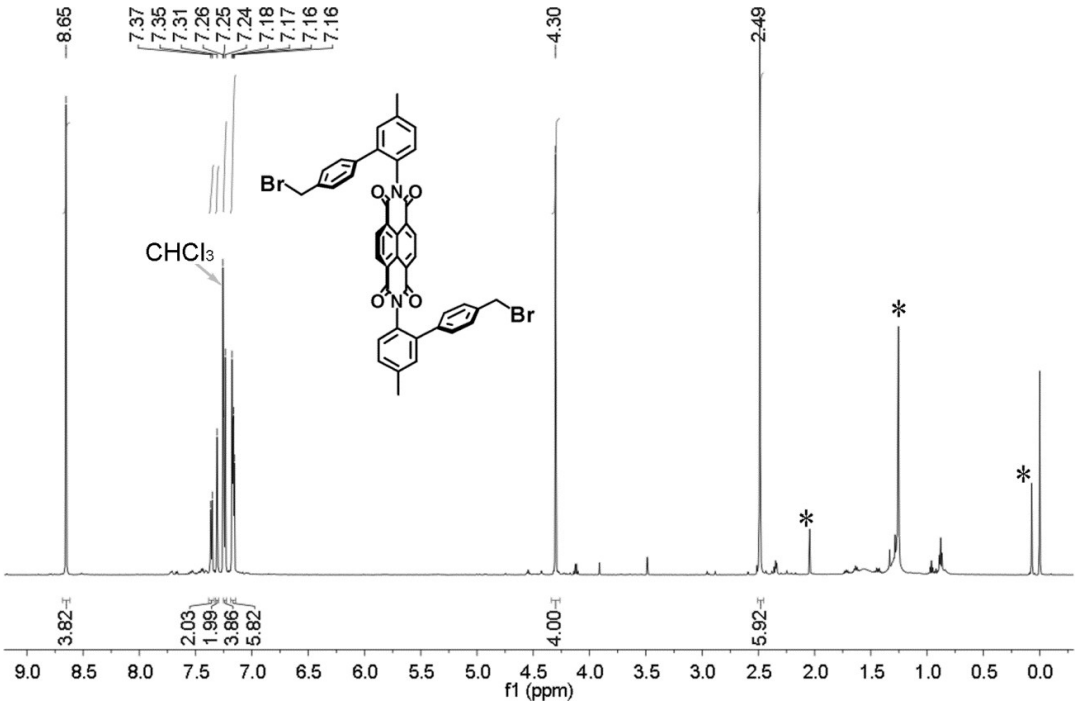

Fig. S3. ^{1}H NMR spectrum of *anti*-**A** in $CDCl_3$. The signals of small amounts of impurities are marked with *.

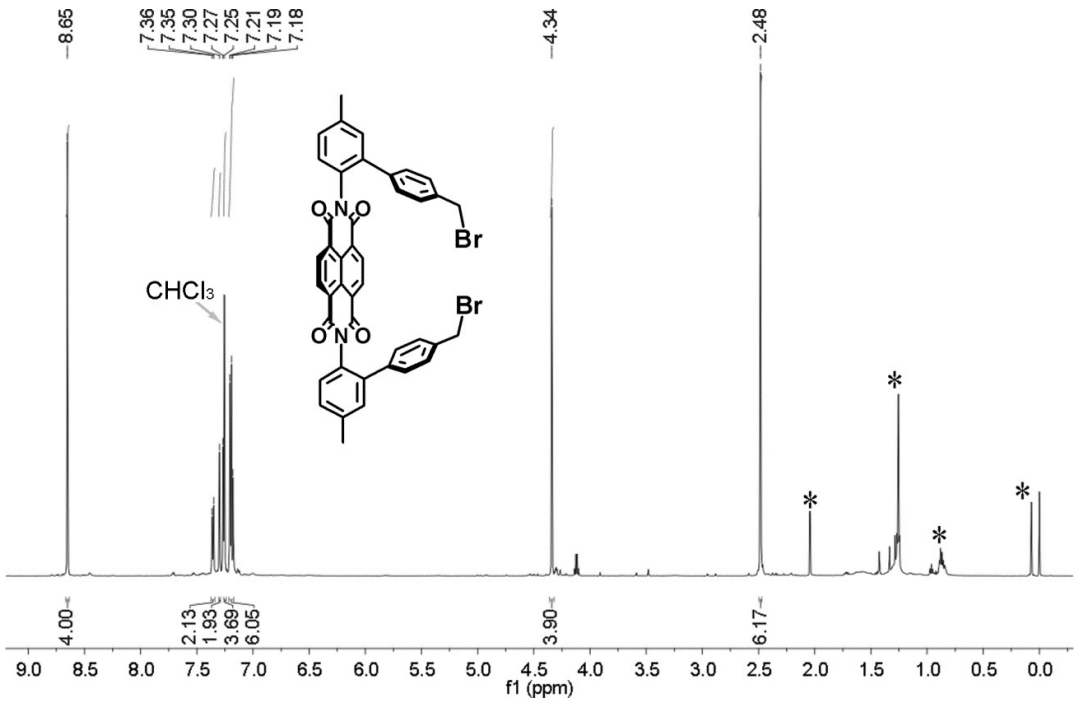

Fig. S4. ^{1}H NMR spectrum of *syn*-**A** in $CDCl_3$. The signals of small amounts of impurities are marked with *.

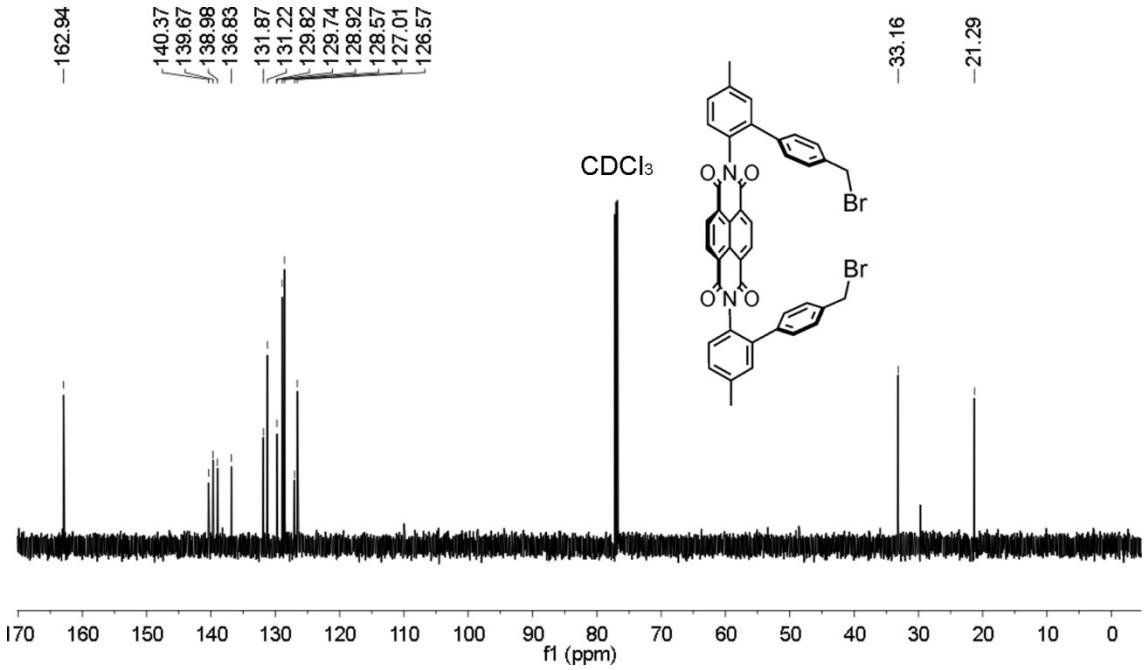

Fig. S5. ^{13}C NMR spectrum of *syn*-**A** in $CDCl_3$.

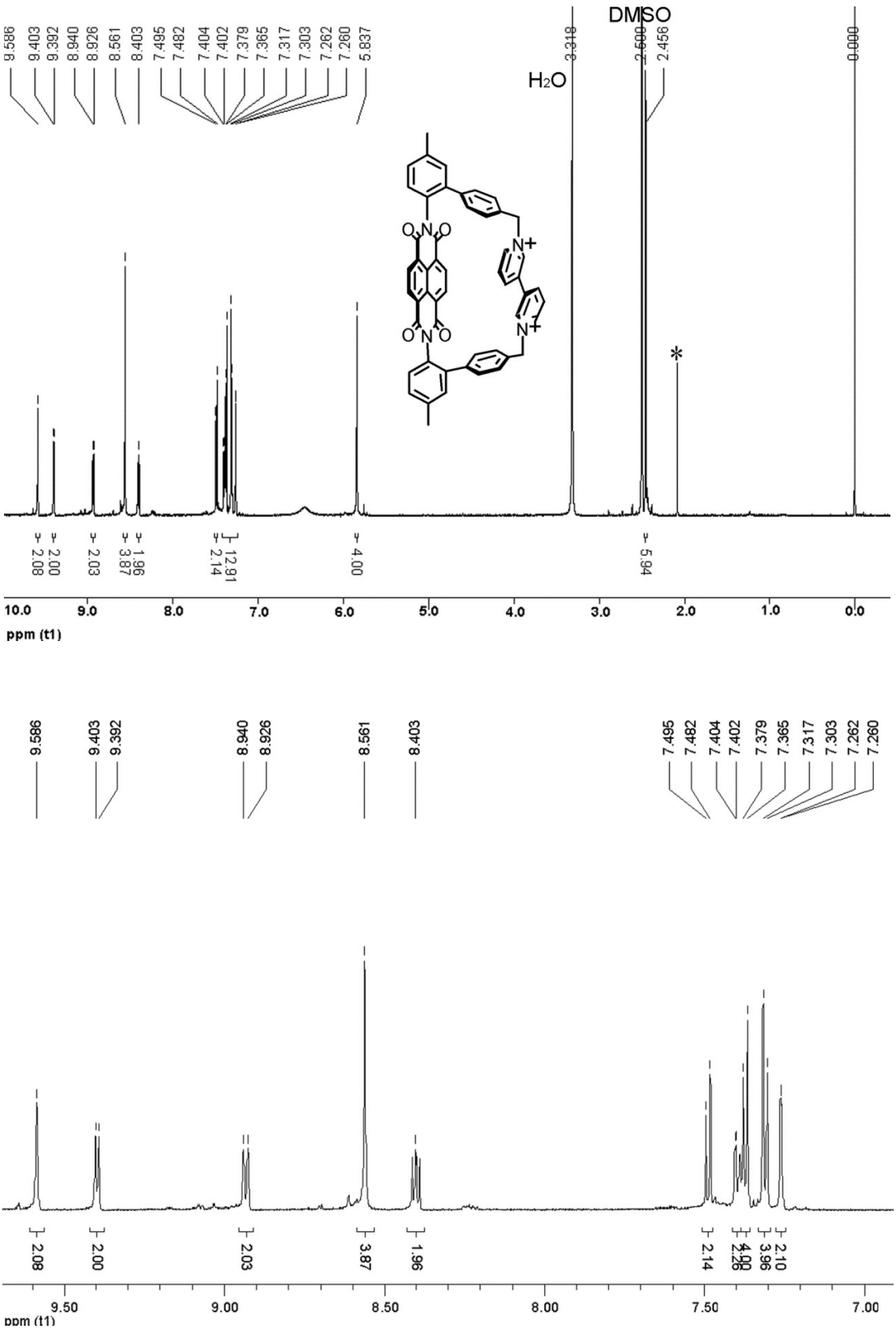

Fig. S6. ^{1}H NMR spectrum of **TBox-1**·2PF$_6$ in DMSO-d$_6$. Top: Full spectrum; Bottom: Partial spectrum. The signals of small amounts of impurities are marked with *.

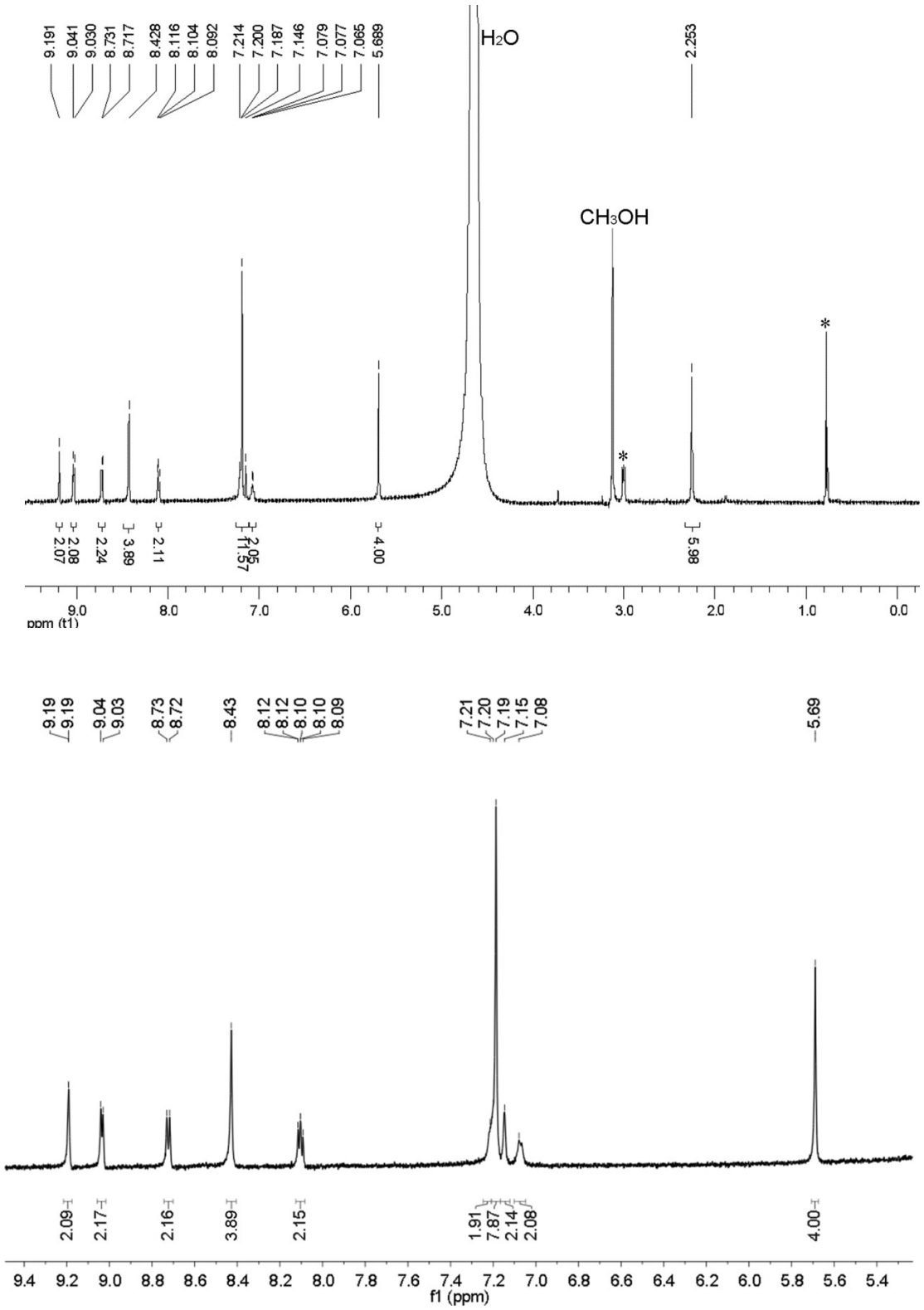

Fig. S7. ^{1}H NMR spectrum of **TBox-1**·2Cl in a mixed D_2O / CD_3OD solution (2:1, v/v). Top: Full spectrum; Bottom: Partial spectrum. The signals of small amounts of impurities are marked with *.

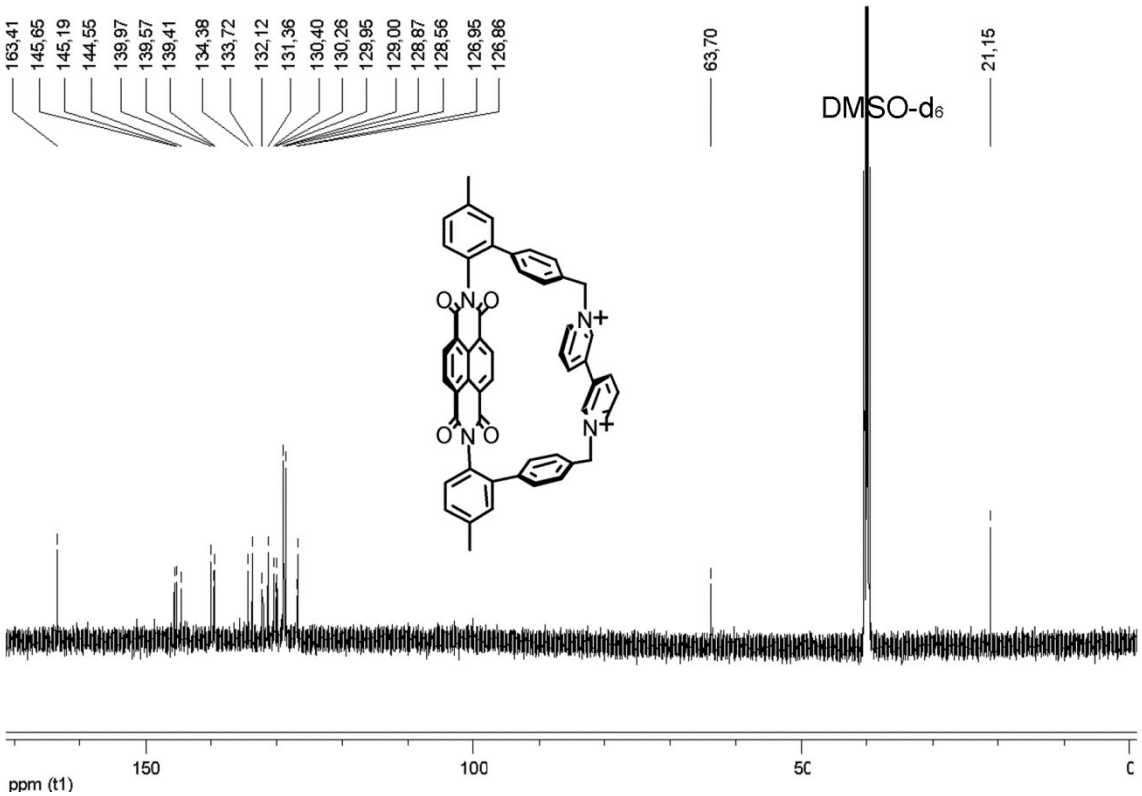

Fig. S8. ^{13}C NMR spectrum of **TBox-1**·$2PF_6$ in DMSO-d_6.

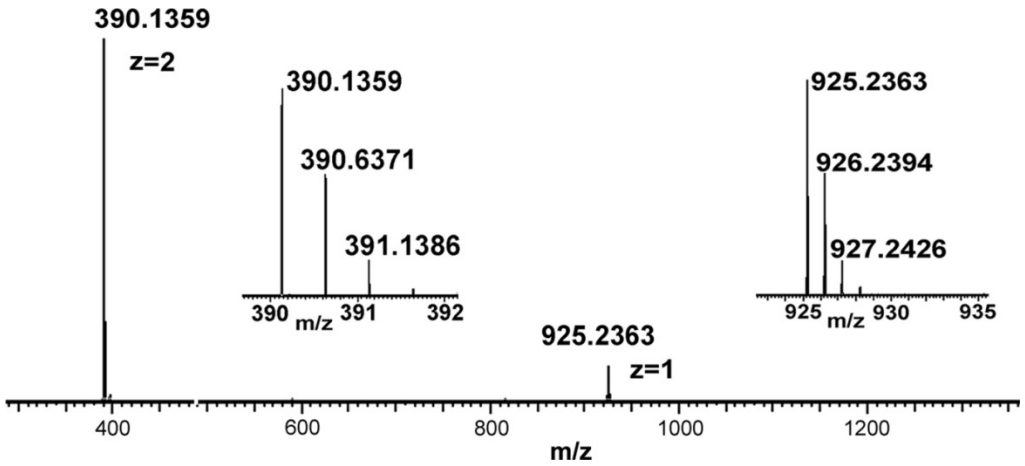

Fig. S9. High resolution ESI-MS of **Tbox-1**·$2PF_6$.

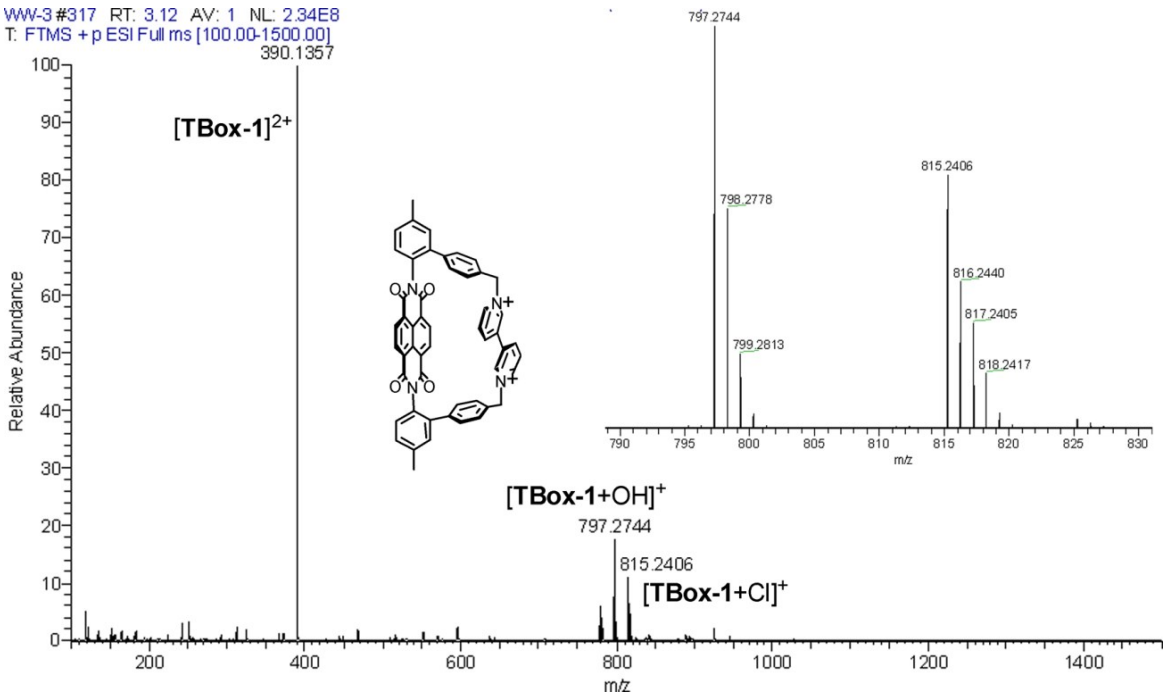

Fig. S10. High resolution ESI-MS of **Tbox-1**·2Cl

1.3 Synthetic Routes of TBox-2.

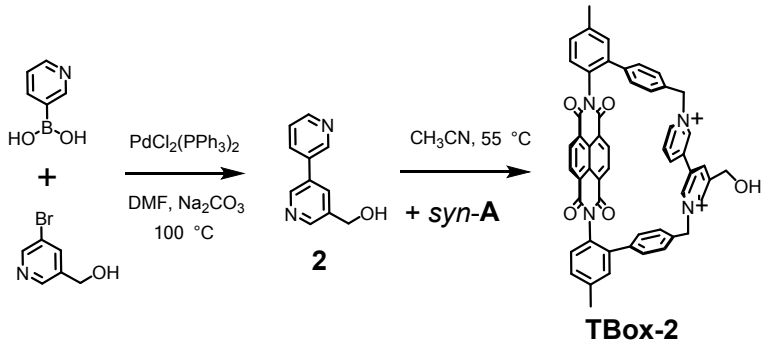

TBox-2

Synthesis of 2:

The solution of 3-bromo-5-hydroxymethylpyridine (0.5 g, 2.66 mmol) in DMF (15 mL) was degassed with nitrogen for 15 min followed by addition of satd Na_2CO_3 solution (5 mL, 2 M) under continuous flow of nitrogen. After 10 min, 3-pyridylboronic acid (0.392 g, 3.19 mmol) and $PdCl_2(PPh_3)_2$ (0.128 g, 0.183 mmol) were added to the reaction mixture under a nitrogen atmosphere. The reaction mixture was stirred at 100 °C for 4 h. The solution was diluted with H_2O (5 mL), and then the product was extracted three times with EtOAc (10 mL). The combined organic layer was dried over $MgSO_4$ and the solvent was removed in vacuo. The crude product was purified on a silica gel column using ethyl acetate as eluent to afford the product as yellow liquid (0.35 g, 71%). **2**: ^{1}H NMR (600 MHz, $CDCl_3$, 298 K): δ (ppm) = 8.819 (s, 1H), 8.744 (s, 1H), 8.649 (d, *J* = 4.8 Hz, 1H), 8.633 (s, 1H), 7.950 (s, 1H), 7.903 (d, *J* = 8.4 Hz, 1H), 7.424 (dd, *J* = 7.8 Hz, 1H), 4.850 (s, 2H); ^{13}C NMR (150 MHz, $CDCl_3$, 298 K): δ (ppm) = 149.06, 147.83, 147.75, 146.75, 137.19, 134.65, 133.40, 133.28, 133.25, 123.90 (C of bipyridine), 62.01 (C of methylene in phenylmethanol).

Synthesis of Tbox-2:

Syn-**A** (203 mg, 0.26 mmol) and **2** (48 mg, 0.26 mmol) were stirred in dry CH_3CN at 55 °C for 6 h under nitrogen protection. The yellow precipitate was collected by vacuum filtration and dissolved in H_2O. When a satd aqueous solution of NH_4PF_6 was added to the reaction mixture, the resulting precipitate was filtered off and then washed with H_2O. The precipitate was dried to afford **TBox-2**·$2PF_6$ (154 mg, 55%) as a yellowish solid. **TBox-2**·$2PF_6$: ^{1}H NMR (600 MHz, DMSO-d_6, 298 K): δ (ppm) = 9.598 (s, 1H), 9.483 (s, 1H), 9.412 (d, *J* = 0.6 Hz, 1H), 9.333 (s, 1H), 8.905 (d, *J* = 7.8 Hz, 1H), 8.854 (s, 1H), 8.561 (s, 4H), 8.394 (t, *J* = 7.2 Hz, 1H), 7.488 (d,

J = 7.8 Hz, 2H), 7.403 (d, J = 7.8 Hz, 2H), 7.402 (d, J = 8.4 Hz, 4H), 7.312 (d, J = 8.4 Hz, 4H), 7.259 (s, 2H), 5.838 (s, 4H), 4.799 (s, 2H), 2.456 (s, 6H); ^{13}C NMR (150 MHz, DMSO-d_6, 298 K): δ (ppm) = 162.72, 145.59, 145.12, 144.48, 144.43, 143.58, 143.06, 142.09, 140.02, 139.99, 139.41, 134.49, 133.90, 133.73, 132.16, 131.37, 130.66, 130.42, 129.95, 129.14, 128.98, 128.89, 128.72, 126.83 (C of aromatic rings), 63.71, 60.02 (C of methylene groups), 21.15 (C of methyl). ESI-MS *m/z* calcd for [**TBox-2**]$^{2+}$: 405.1400, found: 405.1412 (100%).

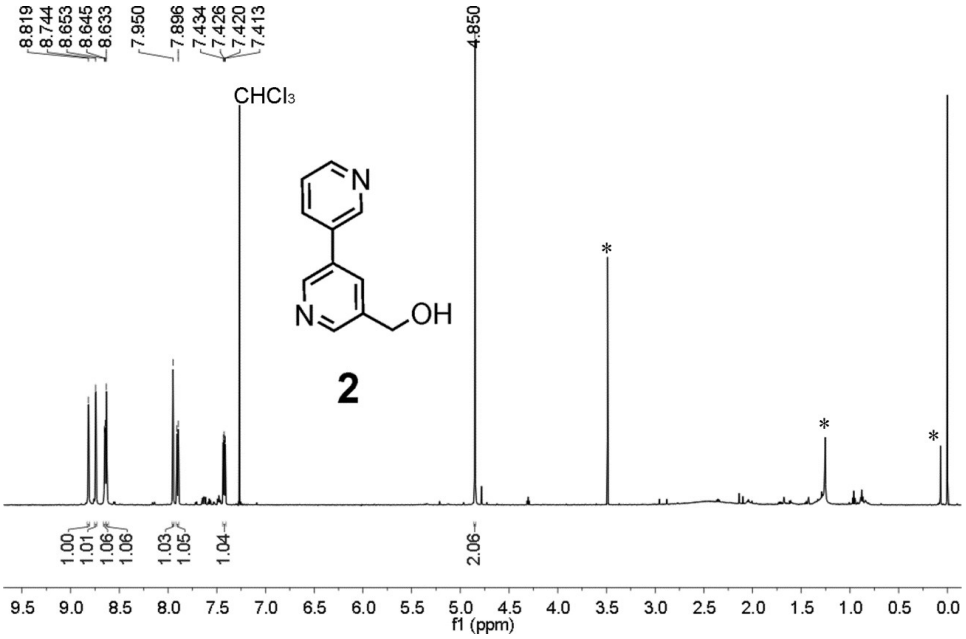

Fig. S11. ^{1}H NMR spectrum of **2** in $CDCl_3$.

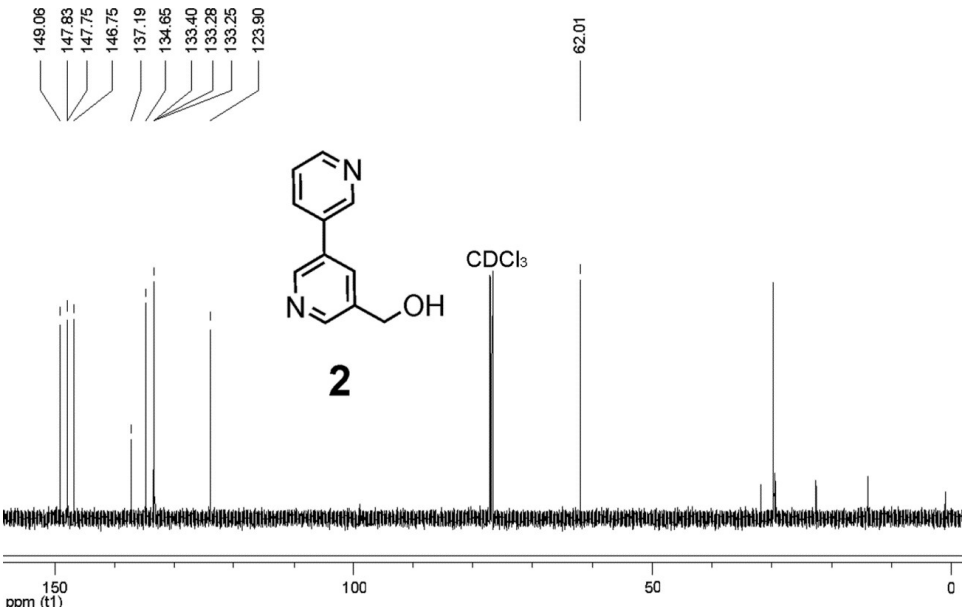

Fig. S12. ^{13}C NMR spectrum of **2** in $CDCl_3$.

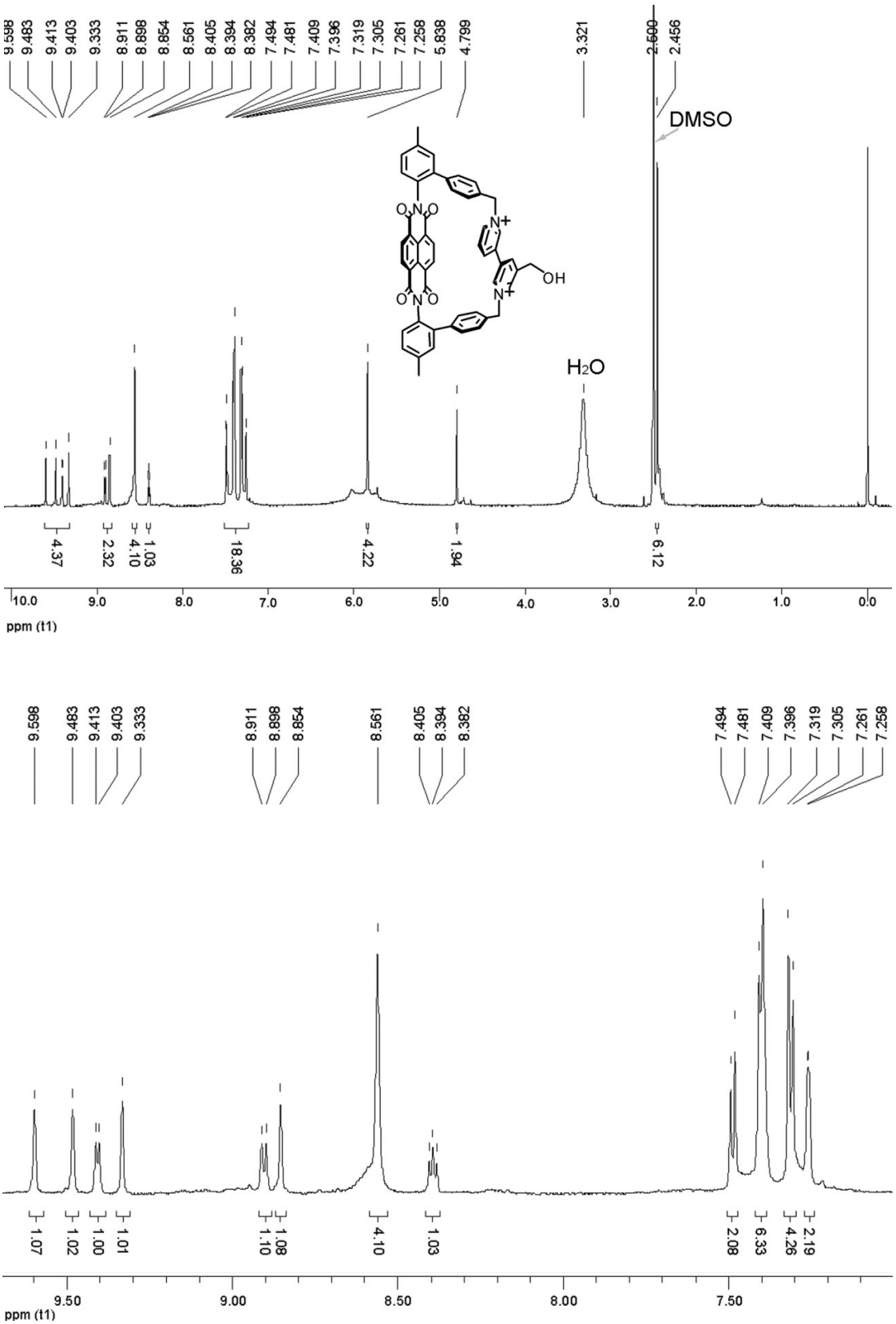

Fig. S13. ^{1}H NMR spectrum of **TBox-2**·2PF_6 in DMSO-d_6. Top: Full spectrum; Bottom: Partial spectrum.

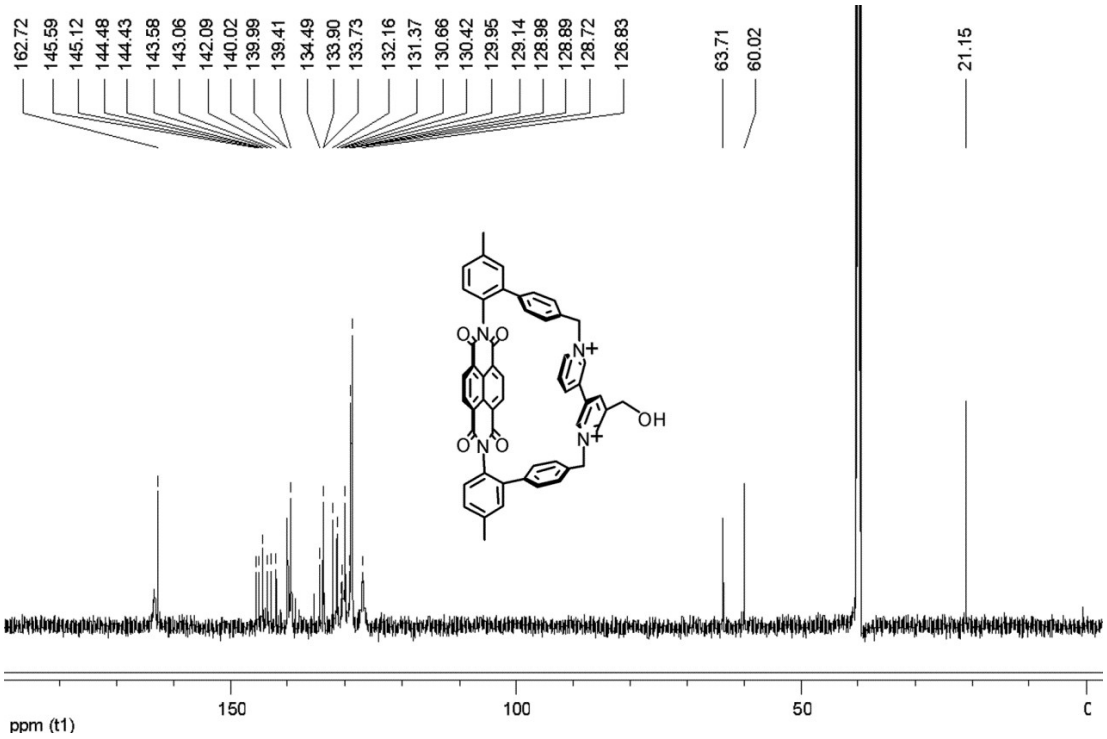

Fig. S14. ^{13}C NMR spectrum of **TBox-2**·2PF$_6$ in DMSO-d$_6$.

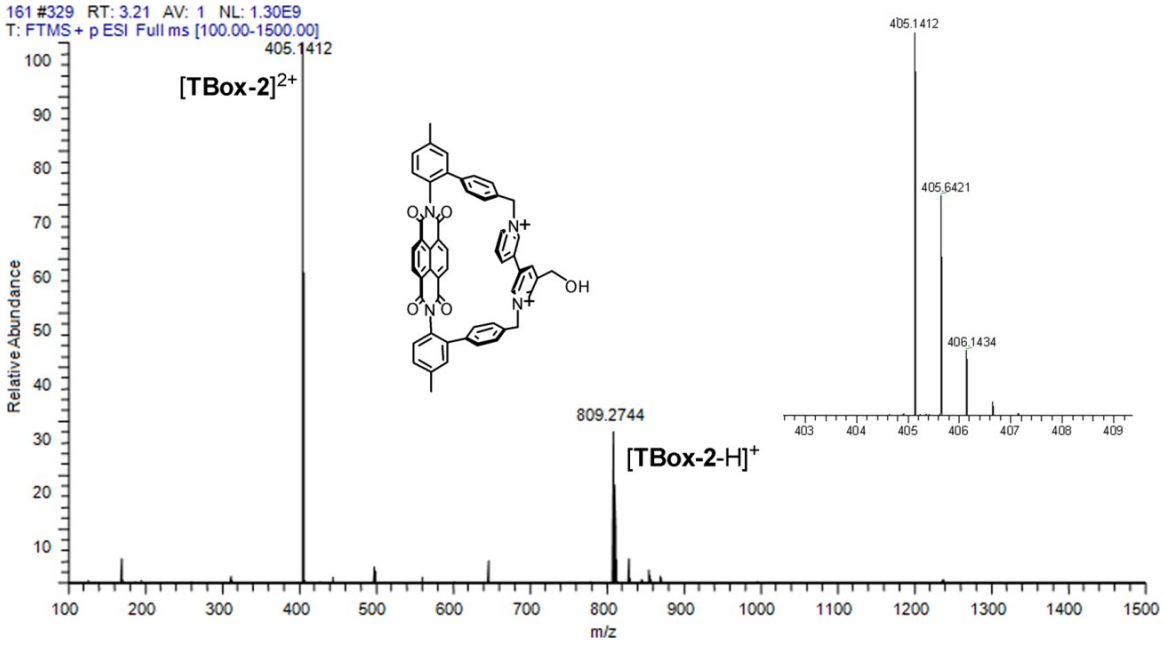

Fig. S15. High resolution ESI-MS of **TBox-2**·2PF$_6$.

1.4 Synthetic Routes of TBox-3.

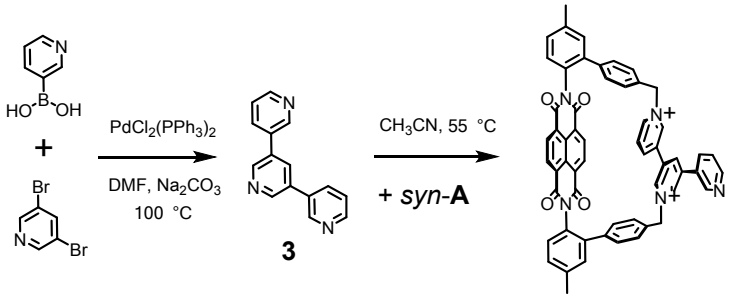

Synthesis of 3:

The solution of 3,5-dibromopyridine (0.63 g, 2.659 mmol) in DMF (15 mL) was degassed with nitrogen for 15 min followed by addition of Na_2CO_3 solution (5 mL, 2 M). After 10 min, 3-pyridylboronic acid (0.82 g, 6.647 mmol) and $PdCl_2(PPh_3)_2$ (0.128 g, 0.183 mmol) were added to the reaction mixture under a nitrogen atmosphere. The reaction mixture was stirred at 100 °C for 5 h. The solution was diluted with H_2O (5 mL), and then the product was extracted three times with EtOAc (10 mL). The combined organic layer was dried over $MgSO_4$ and the solvent was removed in vacuo. The crude product was purified on a silica gel column using ethyl acetate as eluent to afford the product as white solid (0.46 g, 74%). **3**: ^{1}H NMR (600 MHz, DMSO-d_6, 298 K): δ (ppm) = 9.104 (s, 2H), 9.017 (s, 2H), 8.665 (d, *J* = 4.8 Hz, 2H), 8.521 (s, 1H), 8.311 (s, *J* = 7.8 Hz, 2H), 7.563 (dd, *J* = 8.4 Hz, 2H); ^{13}C NMR (150 MHz, $CDCl_3$, 298 K): δ (ppm) = 149.61, 148.21, 147.62, 134.56, 133.78, 133.05, 132.89, 123.85 (C of terpyridyl).

Synthesis of Tbox-3:

Syn-**A** (204 mg, 0.26 mmol) and **3** (61 mg, 0.26 mmol) were stirred in dry CH_3CN at 55 °C for 8 h under nitrogen protection. The yellow precipitate was collected by vacuum filtration and dissolved in H_2O. When a satd aqueous solution of NH_4PF_6 was added to the reaction mixture, the resulting precipitate was filtered off and then washed with deionized H_2O. The precipitate was dried to afford **TBox-3**·$2PF_6$ (149 mg, 50%) as a faint yellow solid. **TBox-3**·$2PF_6$: ^{1}H NMR (600 MHz, DMSO-d_6, 298 K): δ (ppm) = 9.899 (s, 1H), 9.695 (s, 1H), 9.599 (s, 1H), 9.432 (d, *J* = 6.0 Hz, 1H), 9.299 (s, 1H), 9.197 (s, 1H), 9.031 (d, *J* = 8.4 Hz, 1H), 8.813 (s, 1H), 8.555 (s, 4H), 8.438 (t, *J* = 6.6 Hz, 1H), 8.385 (d, *J* = 7.2 Hz, 1H), 7.721 (s, 1H), 7.484 (d, *J* = 12.6 Hz, 2H), 7.402 (d, *J* = 6.6 Hz, 4H), 7.327 (d, *J* = 6.6 Hz, 4H), 7.257 (d, *J* = 12.6 Hz,

2H), 7.036 (s, 2H), 5.878 (s, *2*H), 5.849 (s, *2*H), 2.458 (s, 6H). ^{13}C NMR (150 MHz, DMSO-d_6, 298 K): δ (ppm) = 163.42, 151.75, 150.06, 148.95, 148.48, 148.02, 145.73, 145.16, 144.63, 144.00, 142.36, 140.09, 139.82, 139.43, 137.95, 135.80, 135.04, 134.34, 133.88, 133.51, 132.15, 131.36, 130.43, 129.97, 129.24, 128.97, 128.71, 126.84, 124.60 (C of aromatic rings), 63.83 (C of methylene groups), 21.16 (C of methyl). ESI-MS *m/z* calcd for [**TBox-3**]$^{2+}$: 428.6500, found: 428.6491 (100%); *m/z* calcd for [**TBox-3**-H]$^{+}$: 856.2900, found: 856.2899 (100%); *m/z* calcd for [**TBox-3**+F]$^{+}$: 876.3000, found: 876.3008 (100%); *m/z* calcd for [**TBox-3**+PF_6]$^{+}$: 1002.2600, found: 1002.2626 (100%).

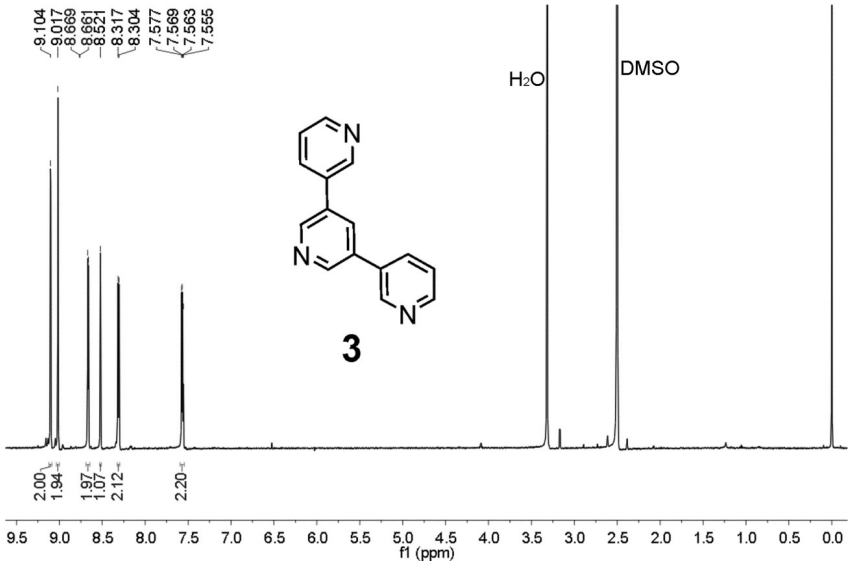

Fig. S16. ^{1}H NMR spectrum of **3** in DMSO-d_6.

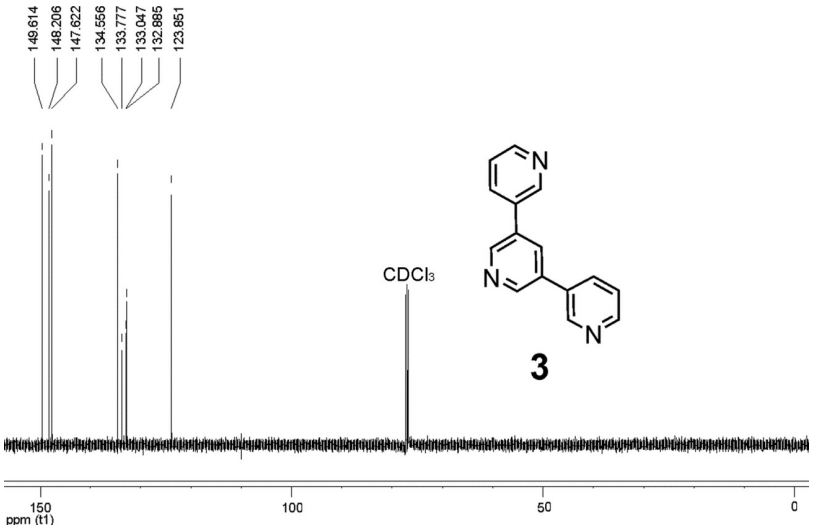

Fig. S17. ^{13}C NMR spectrum of **3** in $CDCl_3$.

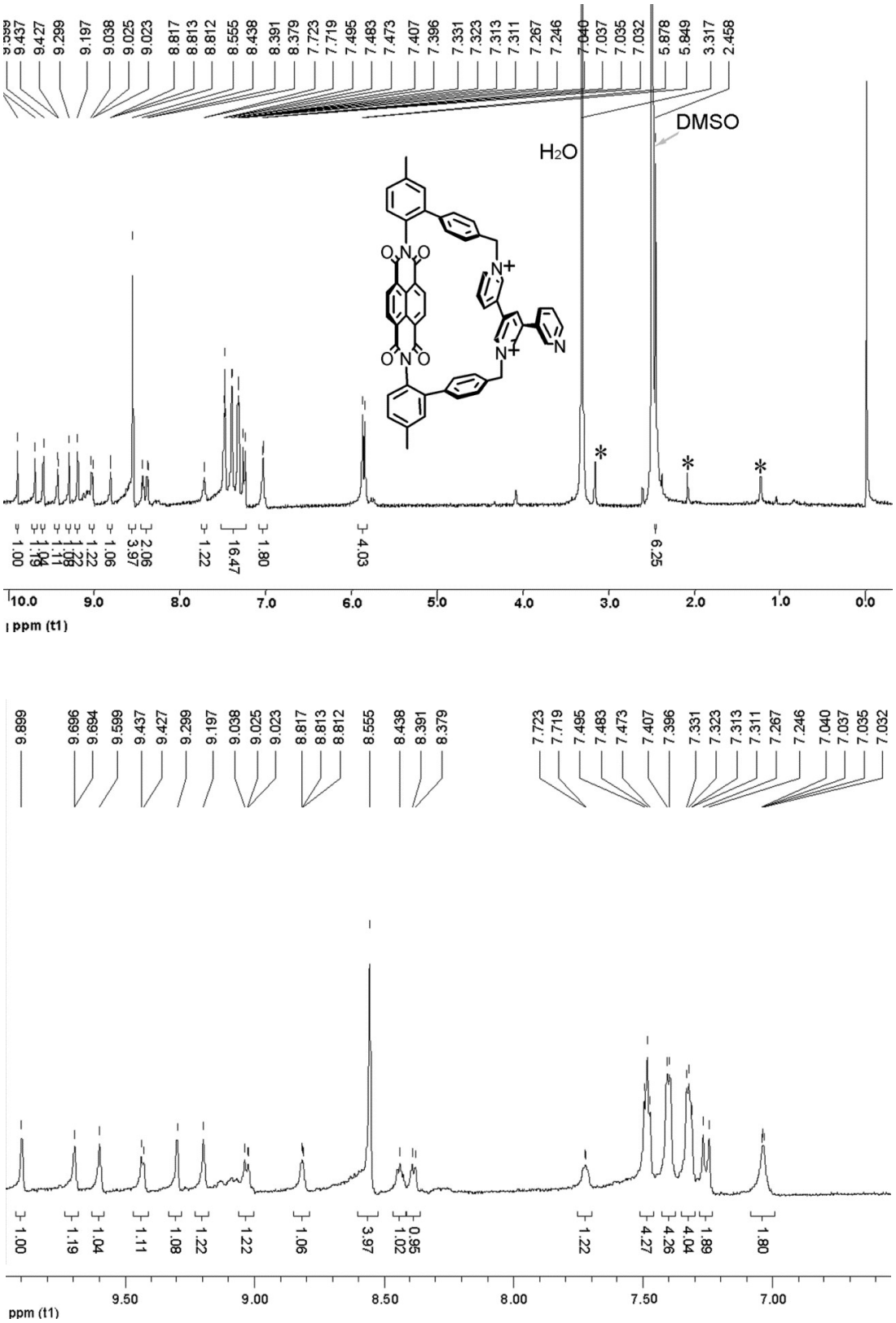

Fig. S18. ^{1}H NMR spectrum of **TBox-3**·2PF_6 in DMSO-d_6. Top: Full spectrum; Bottom: Partial spectrum. The signals of small amounts of impurities are marked with *.

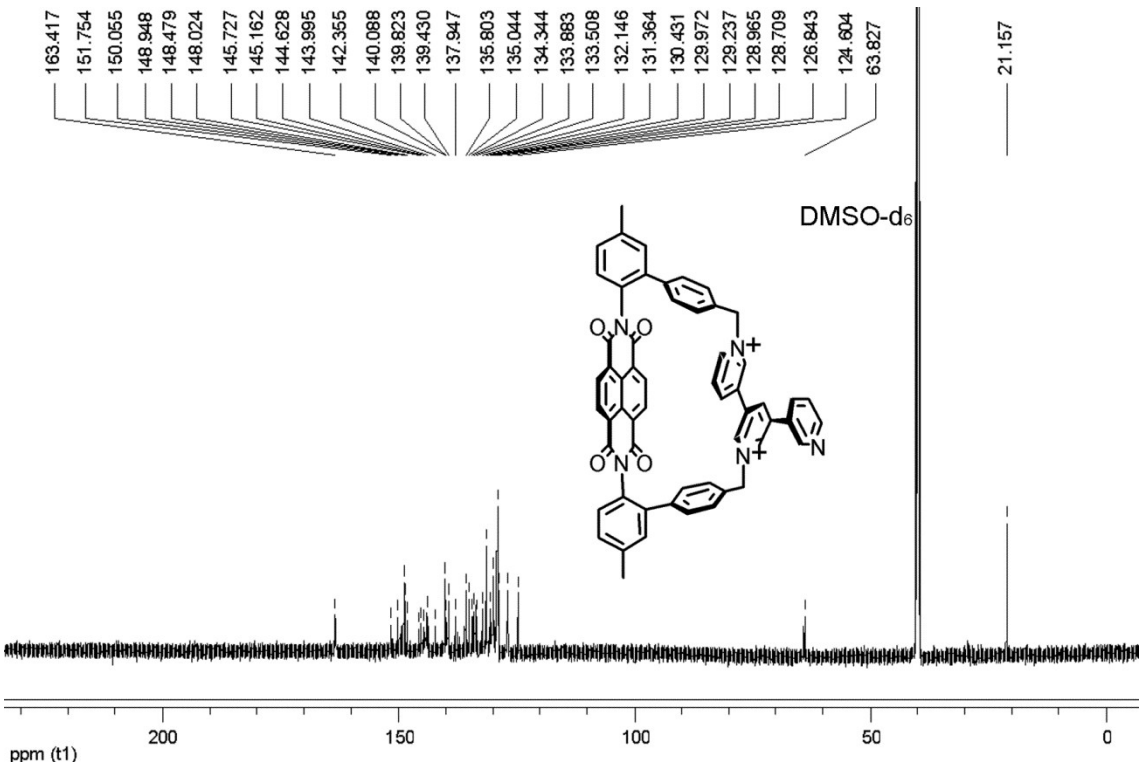

Fig. S19. ^{13}C NMR spectrum of **TBox-3**·2PF$_6$ in DMSO-d$_6$.

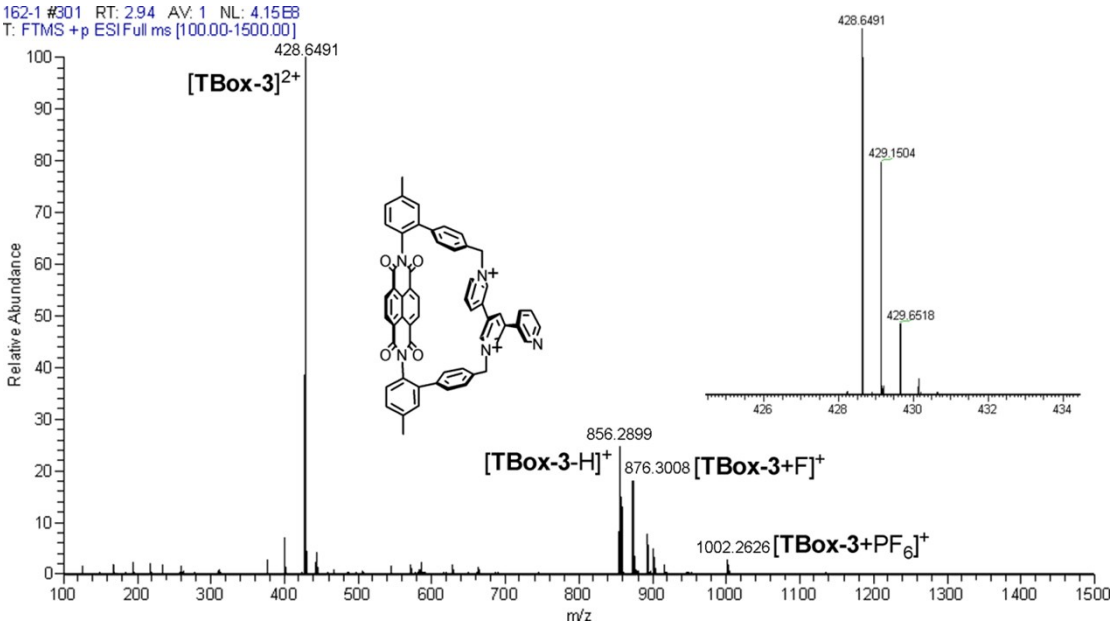

Fig. S20. High resolution ESI-MS of **TBox-3**·2PF$_6$.

2. Determination of Rotational Barrier of Atropisomer Precursor

Anti-**A** (12 mg) was dissolved in deuterated 1,1,2,2-tetrachloroethane (d_2-TCE, 0.6 mL), and was kept at 70 °C. The ratio of the two isomers was determined by standard deconvolution of the methylene protons at 4.375 ppm for *anti*-**A** and 4.348 ppm for *syn*-**A**. The ln[(R-R_e)/(R+1) of was plotted versus time (s), where R_e is the ratio of *anti*/*syn* isomers at equilibrium and R the ratio of *anti*/*syn* at time t seconds. The slope of this plot corresponds to the observed rate k_{obs}, where k_{obs} is equal to 4k, and k is the rate of rotation of a single rotor for a reversible reaction. The 4 accounts for the reversibility of the system (the forward and the reverse rate constants) and the two rotors. Then using the Eyring equation $k = \frac{k_B T}{h} e^{-\frac{\Delta G^{\ddagger}}{RT}}$, the rotational barrier can be determined. The energy of rotation was calculated to be 27.81 kcal/mol at 70 °C. The half-life $t_{1/2}$ equals (ln2)/(4k). Thus, $t_{1/2}$ at 80°C is 64 min, while $t_{1/2}$ at 25 °C is ~80 days.

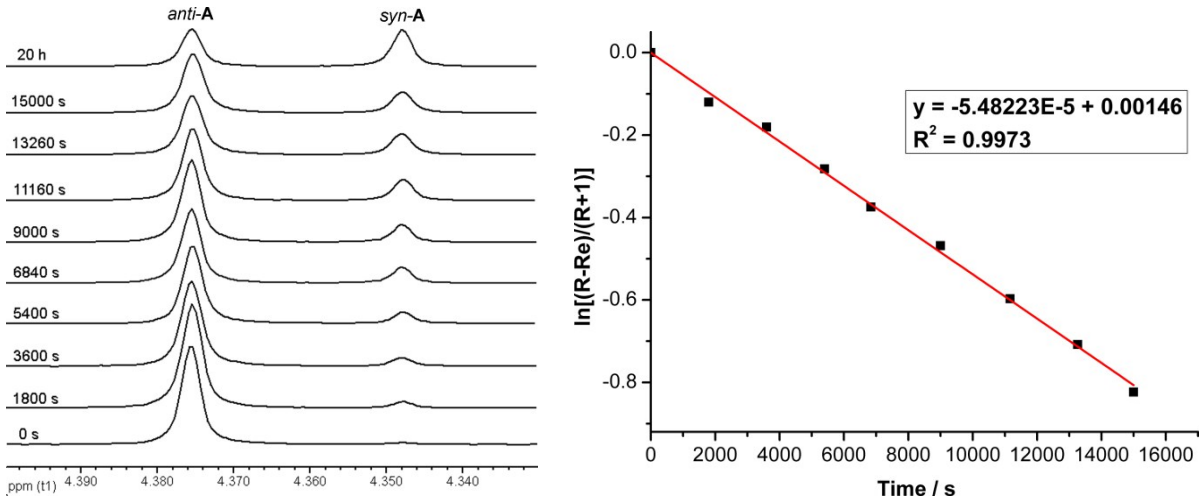

Fig. S21. Left: ^{1}H NMR signals of the methylene protons for *anti*-**A** and *syn*-**A** at 70 °C. Right: Rotational barrier determination via isomeric equilibration.

3. Single Crystal X-Ray Crystallography

Data collections for *anti*-**A**, *syn*-**A** and **Tbox-1** were performed on a Rigaku XtaLAB PRO MM007 diffractometer equipped with a graphite monochromated Cu-Kα radiation (λ = 1.54184 Å) at 173 K. An absorption correction was applied using the SADABS program.[S1] The structures were solved by direct methods and refined on F^2 by full-matrix least-squares using the *SHELXTL*-97 program package. [S2] The ordered atoms in each structure were refined with anisotropic displacement parameters, while the hydrogen atoms were placed in idealized positions and allowed to ride on the relevant carbon atoms. A summary of the crystallographic data of compounds was presented in Table S1. CCDC-1870925 (*anti*-**A**), CCDC-1870926 (*syn*-**A**) and CCDC-1870928 (**Tbox-1**) contain the supplementary crystallographic data for this paper. These data can be obtained free of charge from The Cambridge Crystallographic Data Centre *via* www.ccdc.cam.ac.uk/structures/. Because of the very large thermal motion and disorder of the solvents in the lattice, the diffuse residual electron density is difficult to be accurately modeled and thus a treatment by SQUEEZE (from PLATON) was used for solvate molecule in *syn*-**A**, which leads to large solvent accessible voids in structures. Despite many attempts, the diffraction intensity of **Tbox-1** is very weak, which lead to their high R values and alerts of level A/B in checkCIF reports. Also, H atoms were not located for the four water and two hydroquinone moieties for **Tbox-1**.

Table S1. Crystal data and structure refinements for all the complexes.

	anti-**A**	*syn*-**A**	**Tbox-1**
formula	$C_{24}H_{20}BrNO_3$	$C_{42}H_{28}Br_2N_2O_4$	$C_{64}H_{56}N_4O_{12}P_2F_{12}$
Mr	450.32	784.46	1363.06
Crystal system	triclinic	triclinic	orthorhombic
Space group	*P*-1	*P*-1	*Pccn*
a [Å]	6.1986(3)	10.1328(2)	27.3135(10)
b [Å]	9.7279(4)	12.6924(3)	21.0409(8)
c [Å]	17.3084(9)	15.9749(3)	21.4328(7)
α [°]	87.686(4)	70.388(2)	90
β [°]	83.388(4)	74.964(2)	90
γ [°]	74.340(4)	82.199(2)	90
V [A^3]	998.21(8)	1866.40(7)	12317.4(8)
Z	2	2	8
D_{calcd} [Mg/m^3]	1.498	1.396	1.451
Measured refl.	11416	21243	89868
Unique refl.	3917	7342	7796
R_{int}	0.0539	0.0407	0.2021
GooF	1.080	1.056	1.331
R_1, wR_2 [$I > 2\sigma(I)$]	0.0423, 0.1167	0.0453, 0.1128	0.1380, 0.3548
R_1, wR_2 [all data]	0.0462, 0.1193	0.0482, 0.1150	0.2320, 0.4098

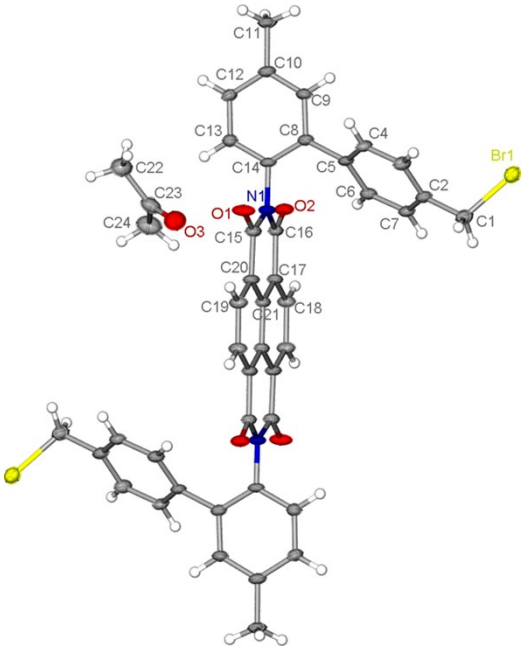

Fig. S22. Single crystal structure of *anti*-**A**. The asymmetric unit has one half of an *anti*-**A** molecule lying about an inversion centre and one molecule of acetone in a general position, and the C, N, O and Br atoms are drawn as 50% thermal ellipsoids.

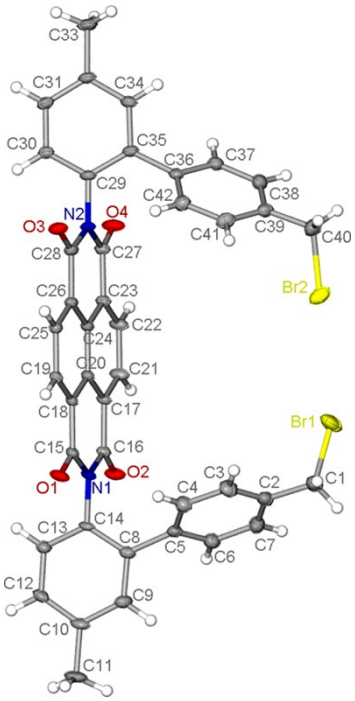

Fig. S23. Single crystal structure of *syn*-**A**. The asymmetric unit has one *syn*-**A** molecule in a general position with no imposed crystallographic symmetry, and the C, N, O and Br atoms are drawn as 50% thermal ellipsoids.

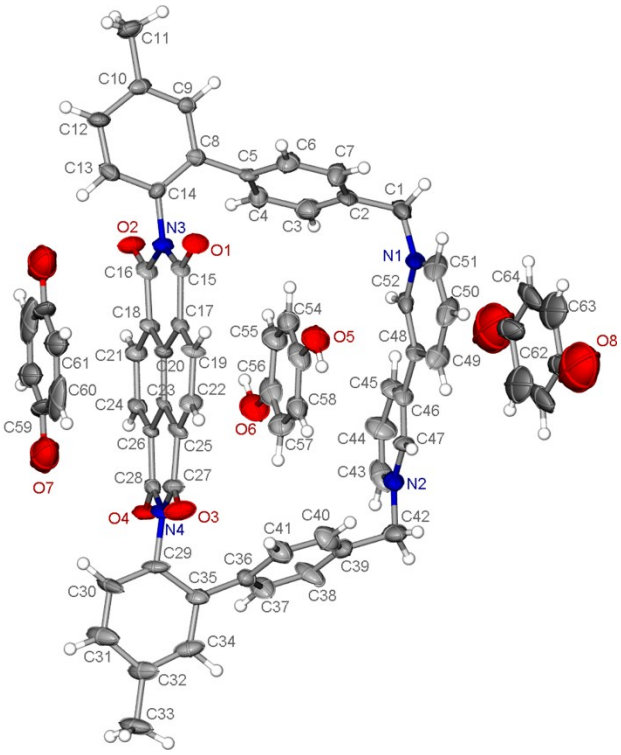

Fig. S24. Single crystal structure of **TBox-1**. The asymmetric unit has one **TBox-1**$^{2+}$ cation in a general position, one hydroquinone molecule in a general position located in the centre of **TBox-1**$^{2+}$, two half quinone molecules lying about inversion centres, one PF_6 ion in a general position, two half PF_6 moieties lying about twofold axes and four water oxygens all in general positions, and the C, N and O atoms are drawn as 30% thermal ellipsoids. Disordered solvents and PF_6^- were omitted for clarity.

4. Characterization of Host-guest Properties

The association constant (K_a) for the formation of the 1:1 complex between guest molecules and **TBox-1** were determined by UV-Vis titration experiments. When the solution of guest was added incrementally to the solution of **TBox**, the UV-Vis spectra were recorded one after the other. The stacked spectra show that, upon the addition of guest, new absorption bands emerge and are enhanced.

Nonlinear curve-fitting method was then used to obtain the association constant through the following equation:

$$\Delta A = \Delta\varepsilon*\{0.5*G_0+0.5*(H_0+1/K_a)-\text{sqrt}[0.25*(H_0+G_0+1/K_a)\text{^}2-H_0*G_0]\}$$

where ΔA is the change in the absorbance on gradual addition of guest, whereas $\Delta\varepsilon$ refers to the difference of molar absorptivity between host-guest complexes and free hosts; the total concentration of **TBox** and guest is denoted by H_0 and G_0. From the UV-vis titration experiments, plots of absorption intensity against the guest concentrations were obtained and nonlinear least squares data treatments (red line) gave the corresponding association constants of host-guest complexes.[S3]

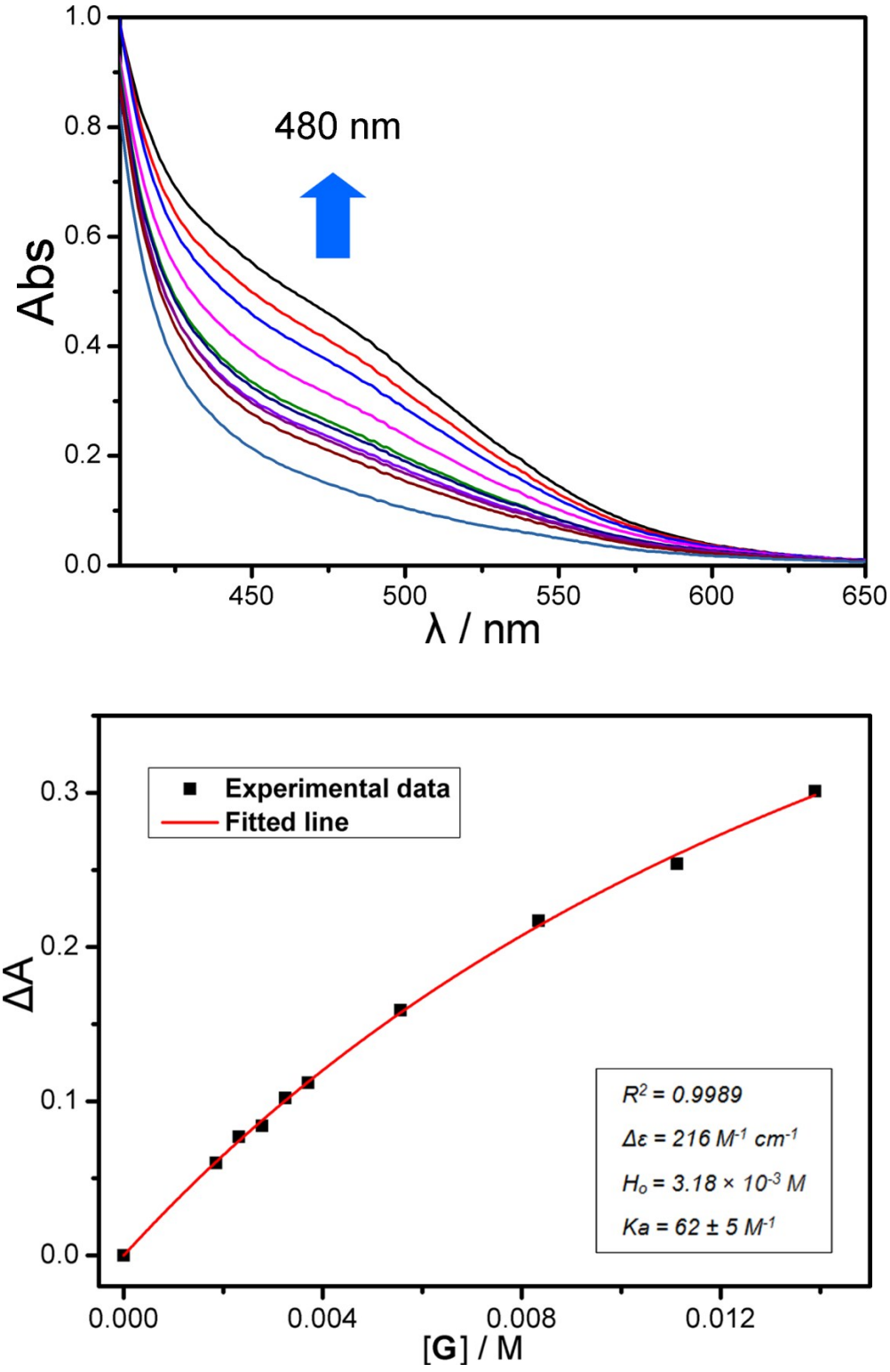

Fig. S25. Top: Stacked UV-Vis spectra obtained by titrating quinol (**G1**) into a CH_3CN solution of **TBox-1**·$2PF_6$ (3.18×10^{-3} M) at 298 K; Bottom: The nonlinear curve-fitting for the complexation of **TBox-1** with **G1** to give an association constant of 62 ± 5 M^{-1}.

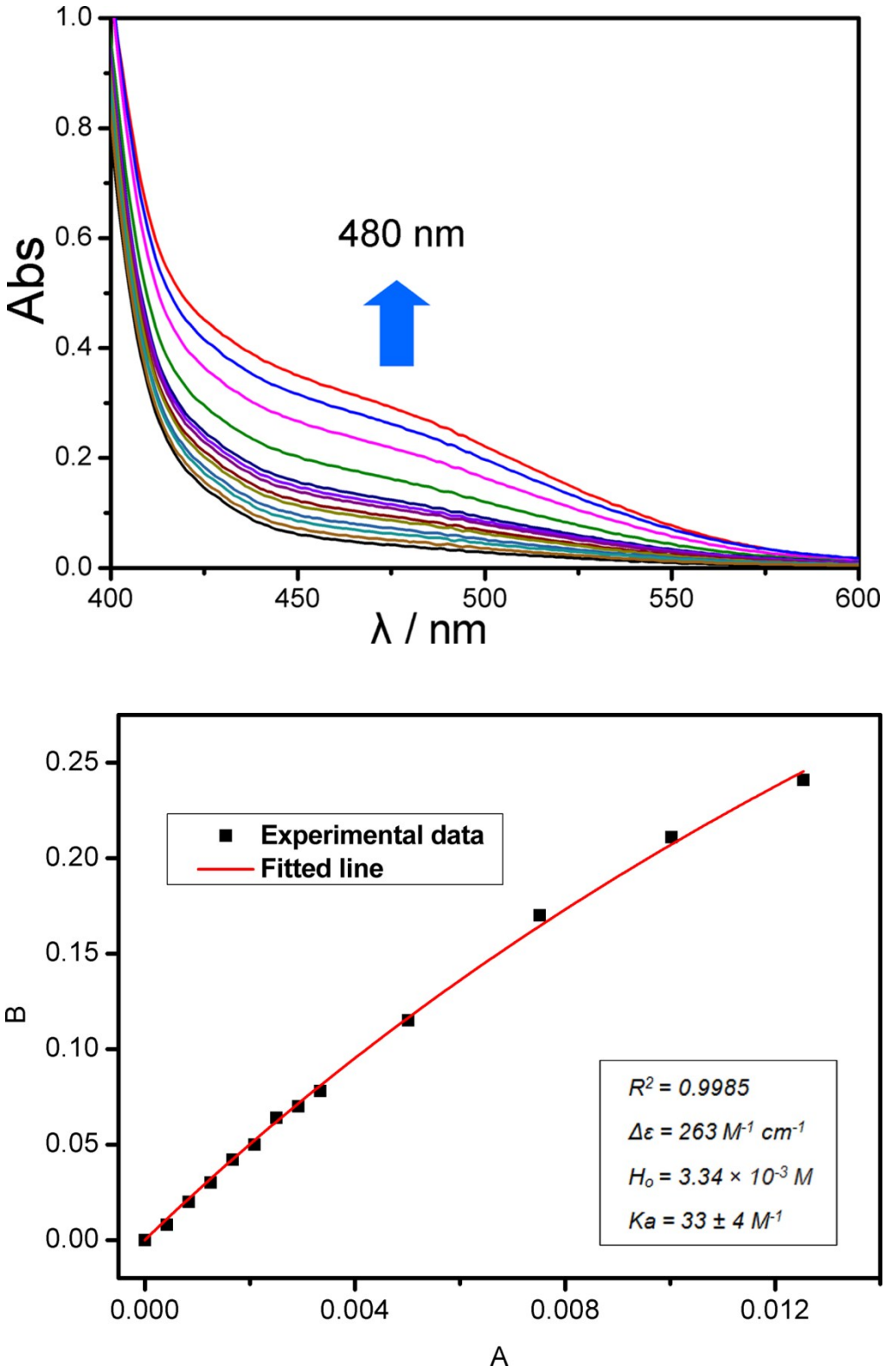

Fig. S26. Top: Stacked UV-Vis spectra obtained by titrating **G1** into a CH_3CN solution of **TBox-2**·$2PF_6$ (3.4×10^{-3} M) at 298 K; Bottom: The nonlinear curve-fitting for the complexation of **TBox-2** with **G1** to give an association constant of 33 ± 4 M^{-1}.

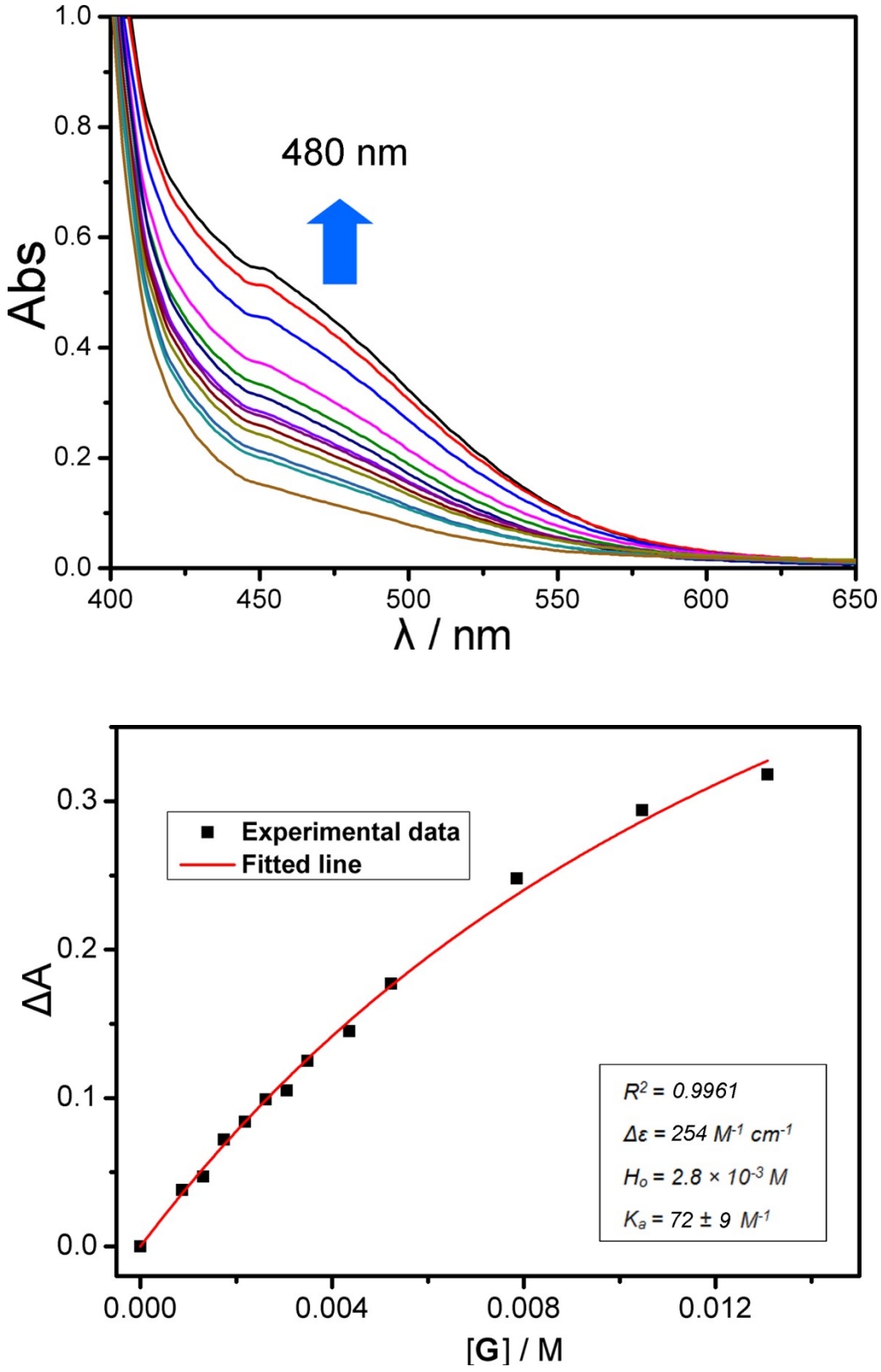

Fig. S27. Top: Stacked UV-Vis spectra obtained by titrating **G1** into a CH_3CN solution of **TBox-3**·$2PF_6$ (2.8×10^{-3} M) at 298 K; Bottom: The nonlinear curve-fitting for the complexation of **TBox-3** with **G1** to give an association constant of 72 ± 9 M^{-1}.

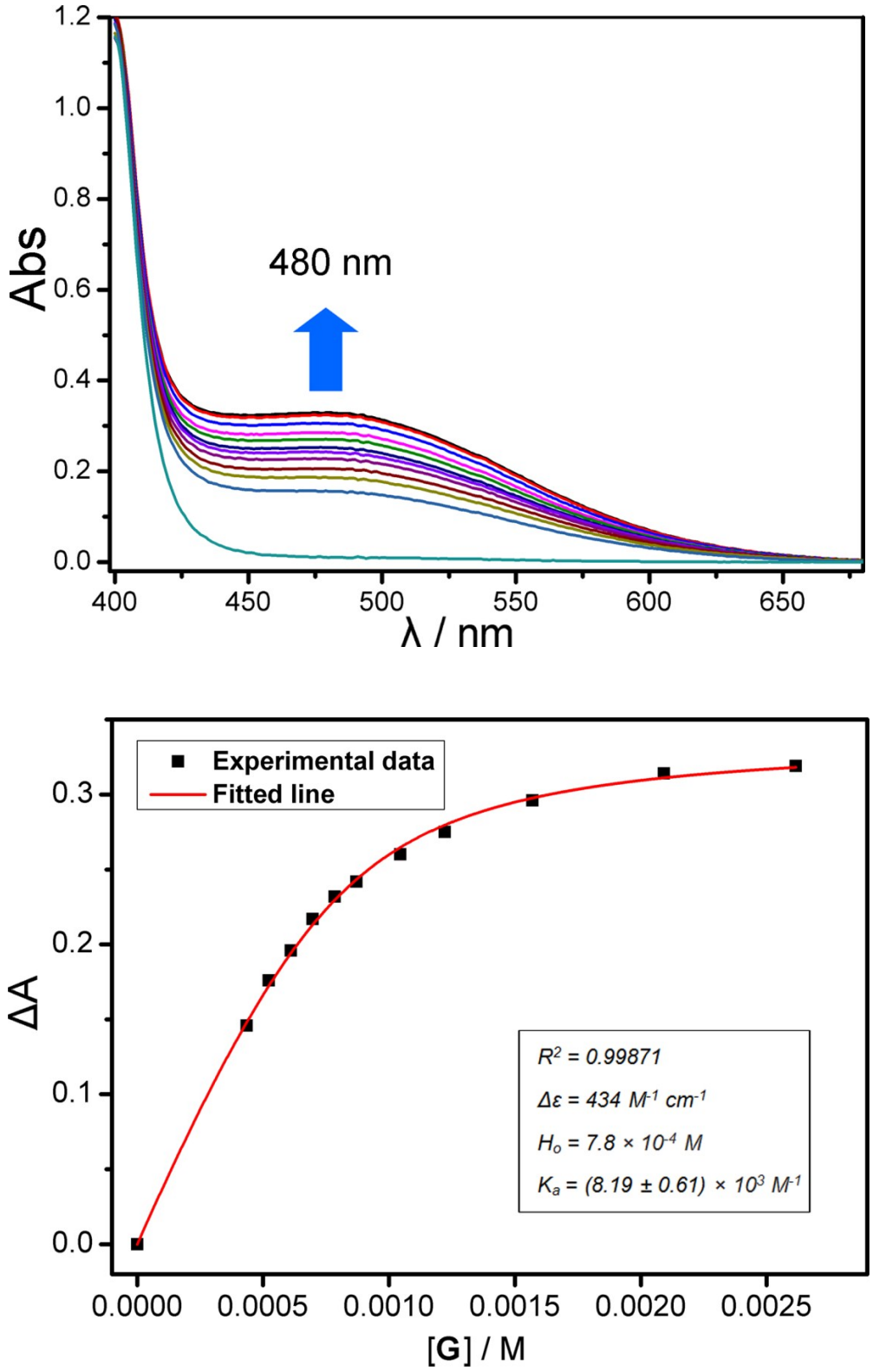

Fig. S28. Top: Stacked UV-Vis spectra obtained by titrating **G1** into a aqueous solution of **TBox-1**·2Cl (7.8×10^{-4} M) at 298 K; Bottom: The nonlinear curve-fitting for the complexation of **TBox-1** with **G1** to give an association constant of $(8.19 \pm 0.61) \times 10^3$ M^{-1}.

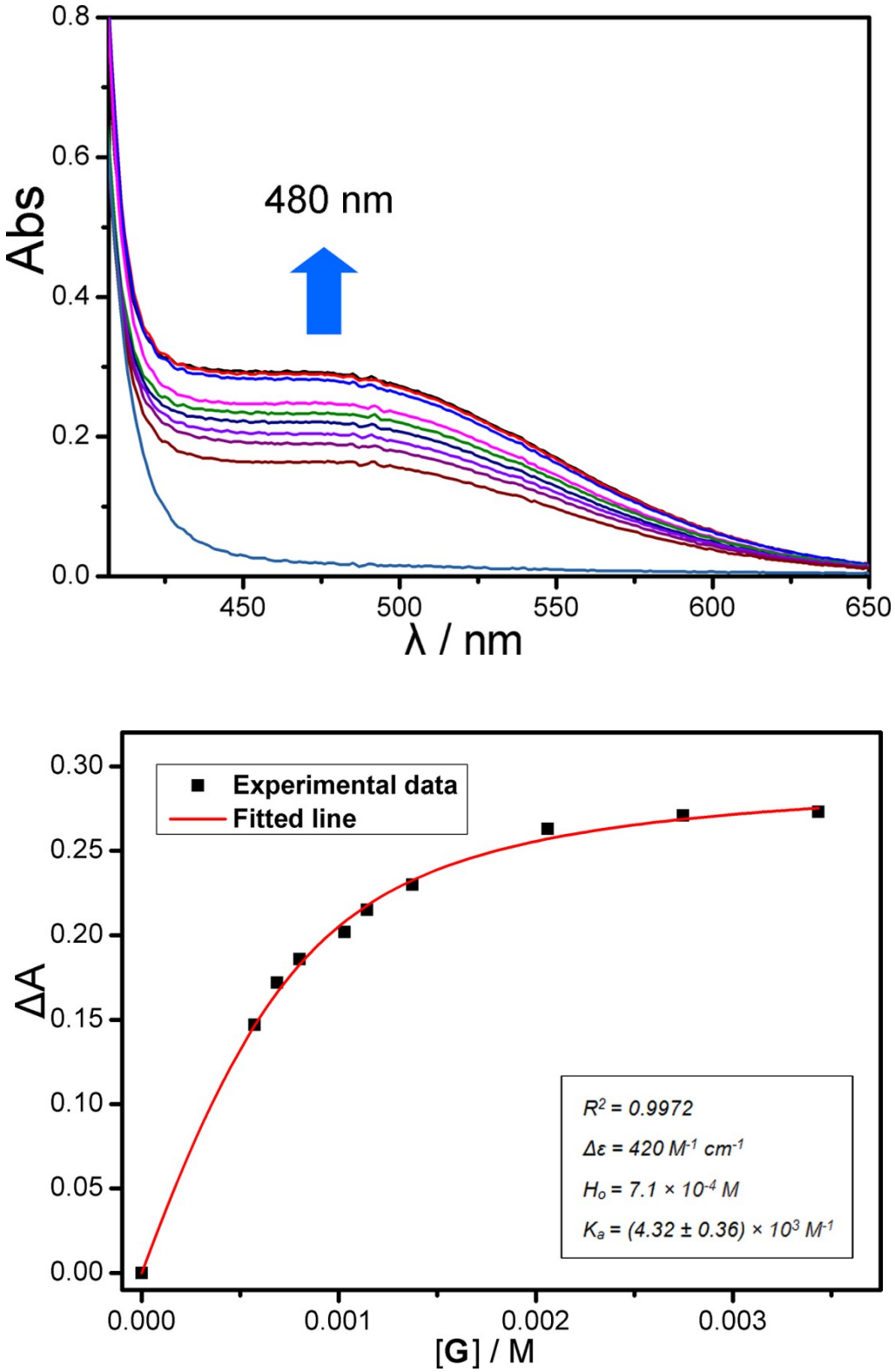

Fig. S29. Top: Stacked UV-Vis spectra obtained by titrating **G1** into a aqueous solution of **TBox-2**·2Cl (7.1×10^{-4} M) at 298 K; Bottom: The nonlinear curve-fitting for the complexation of **TBox-2** with **G1** to give an association constant of $(4.32 \pm 0.36) \times 10^3$ M^{-1}.

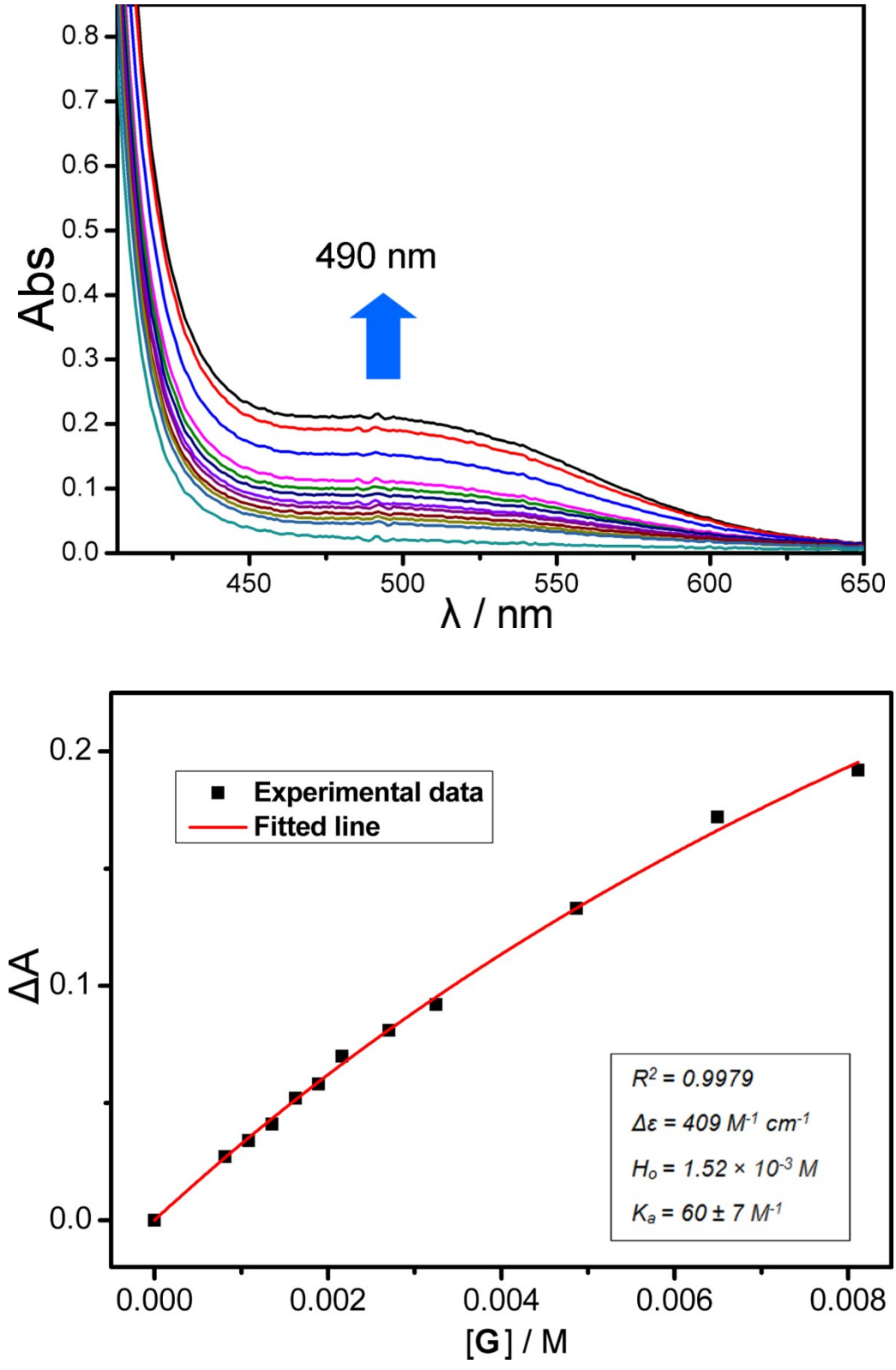

Fig. S30. Top: Stacked UV-Vis spectra obtained by titrating 2,6-naphthalenediol (**G2**) into a CH_3CN solution of **TBox-1**·$2PF_6$ (1.52×10^{-3} M) at 298 K; Bottom: The nonlinear curve-fitting for the complexation of **TBox-1** with **G2** to give an association constant of 60 ± 7 M^{-1}.

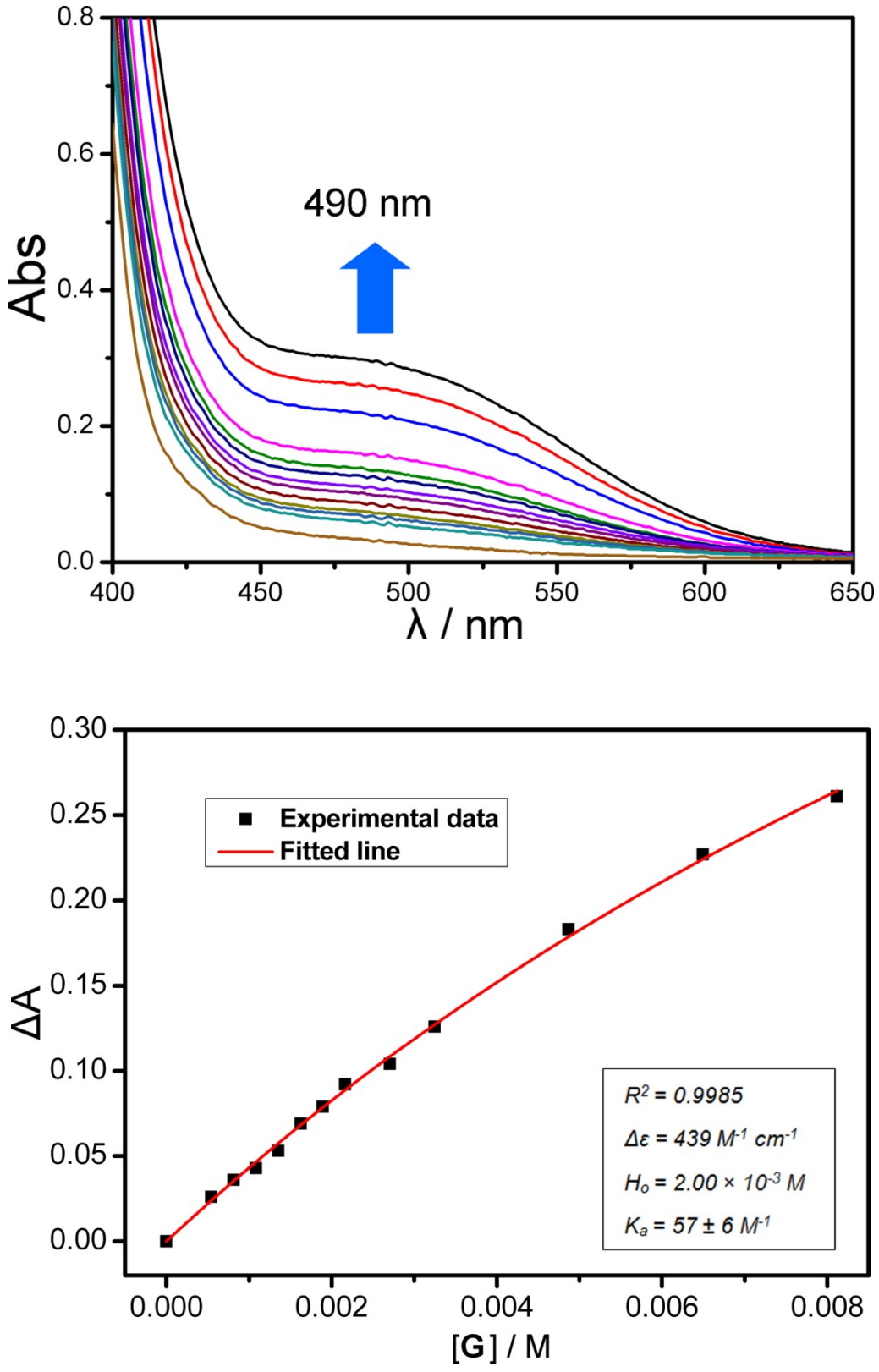

Fig. S31. Top: Stacked UV-Vis spectra obtained by titrating **G2** into a CH_3CN solution of **TBox-2**·$2PF_6$ (2.00×10^{-3} M) at 298 K; Bottom: The nonlinear curve-fitting for the complexation of **TBox-2** with **G2** to give an association constant of 57 ± 6 M^{-1}.

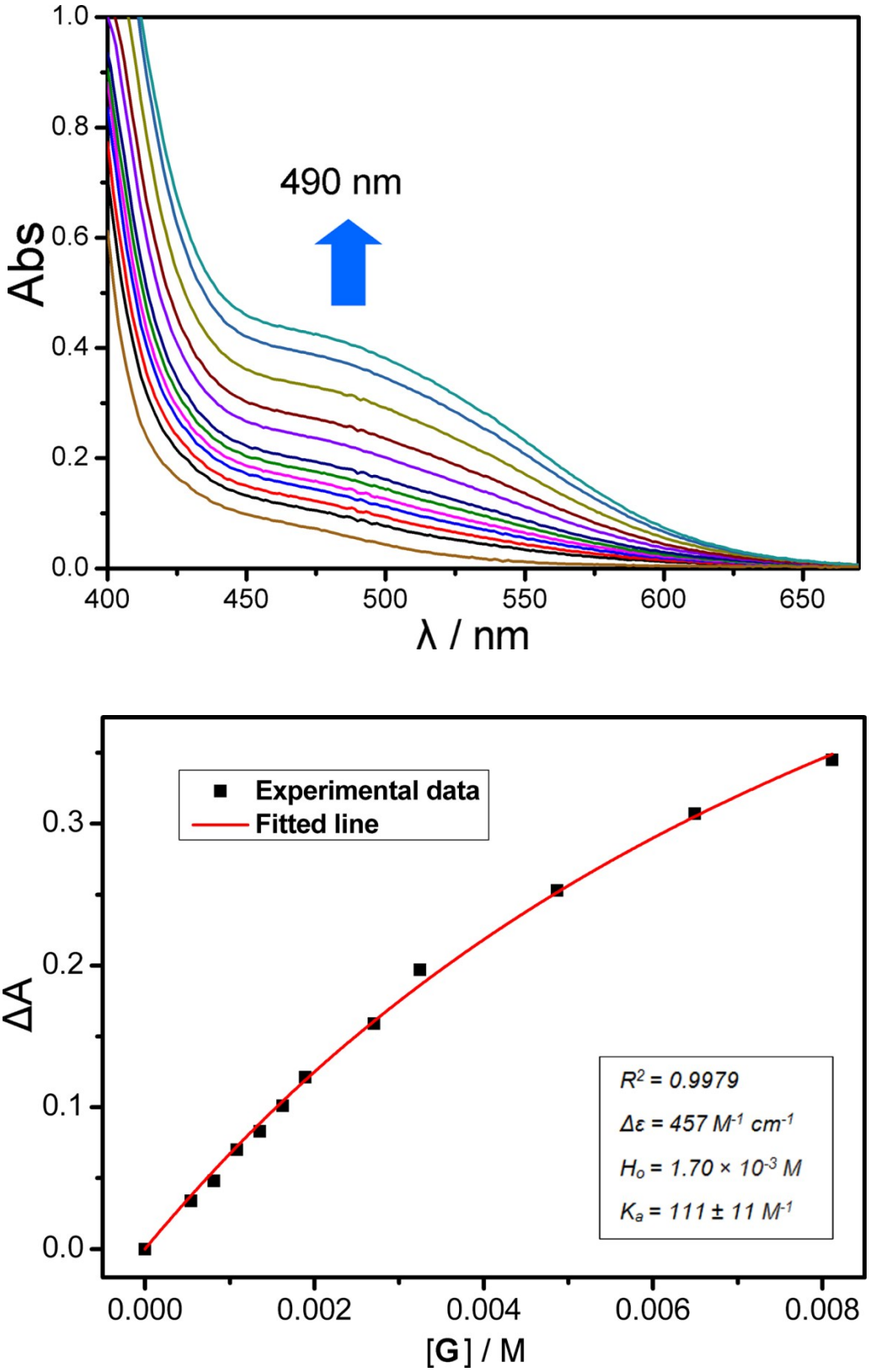

Fig. S32. Top: Stacked UV-Vis spectra obtained by titrating **G2** into a CH_3CN solution of **TBox-3**·$2PF_6$ (1.70×10^{-3} M) at 298 K; Bottom: The nonlinear curve-fitting for the complexation of **TBox-3** with **G2** to give an association constant of 111 ± 11 M^{-1}.

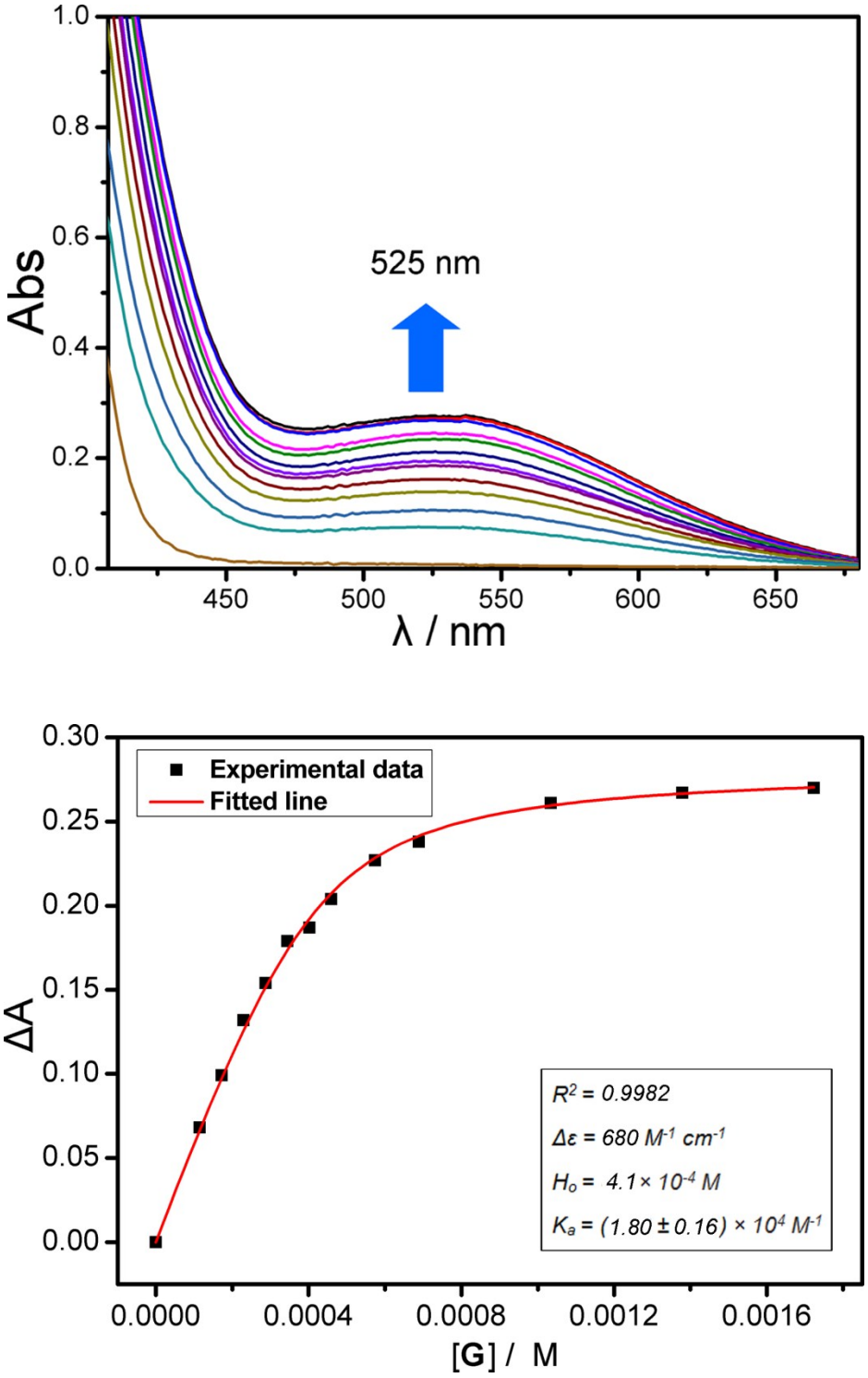

Fig. S33. Top: Stacked UV-Vis spectra obtained by titrating **G2** into a mixed water/methanol solution (11:1, v/v) of **TBox-1**·2Cl (4.1×10^{-4} M) at 298 K. The mixed solution was used because of the low solubility of **G2** in pure water. Bottom: The nonlinear curve-fitting for the complexation of **TBox-1** with **G2** to give an association constant of $(1.80 \pm 0.16) \times 10^4$ M^{-1}.

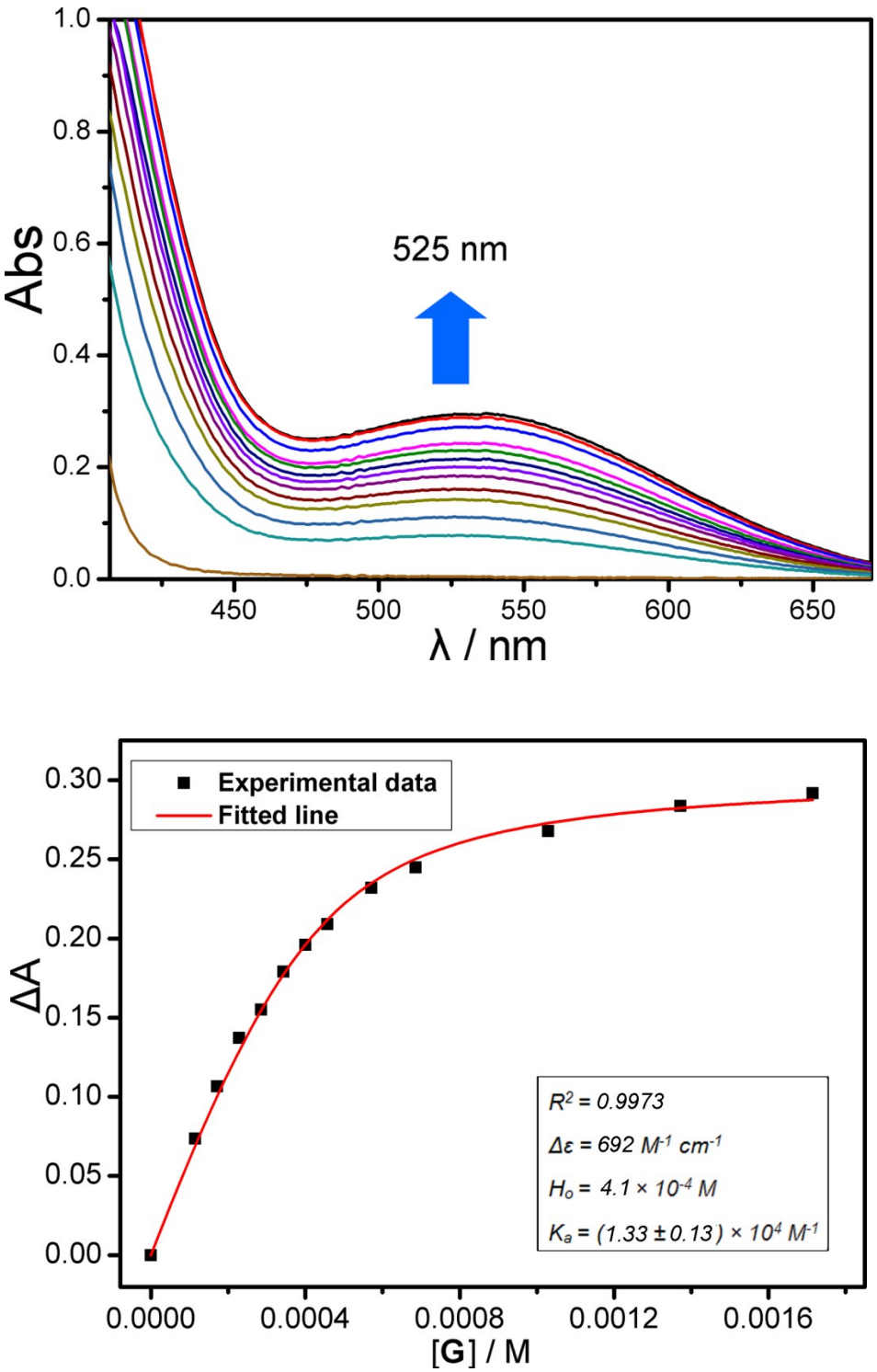

Fig. S34. Top: Stacked UV-Vis spectra obtained by titrating **G2** into a mixed water/methanol solution (11:1, v/v) of **TBox-2**·2Cl (4.1×10^{-4} M) at 298 K. The mixed solution was used because of the low solubility of **G2** in pure water. Bottom: The nonlinear curve-fitting for the complexation of **TBox-2** with **G2** to give an association constant of $(1.33 \pm 0.13) \times 10^4$ M^{-1}.

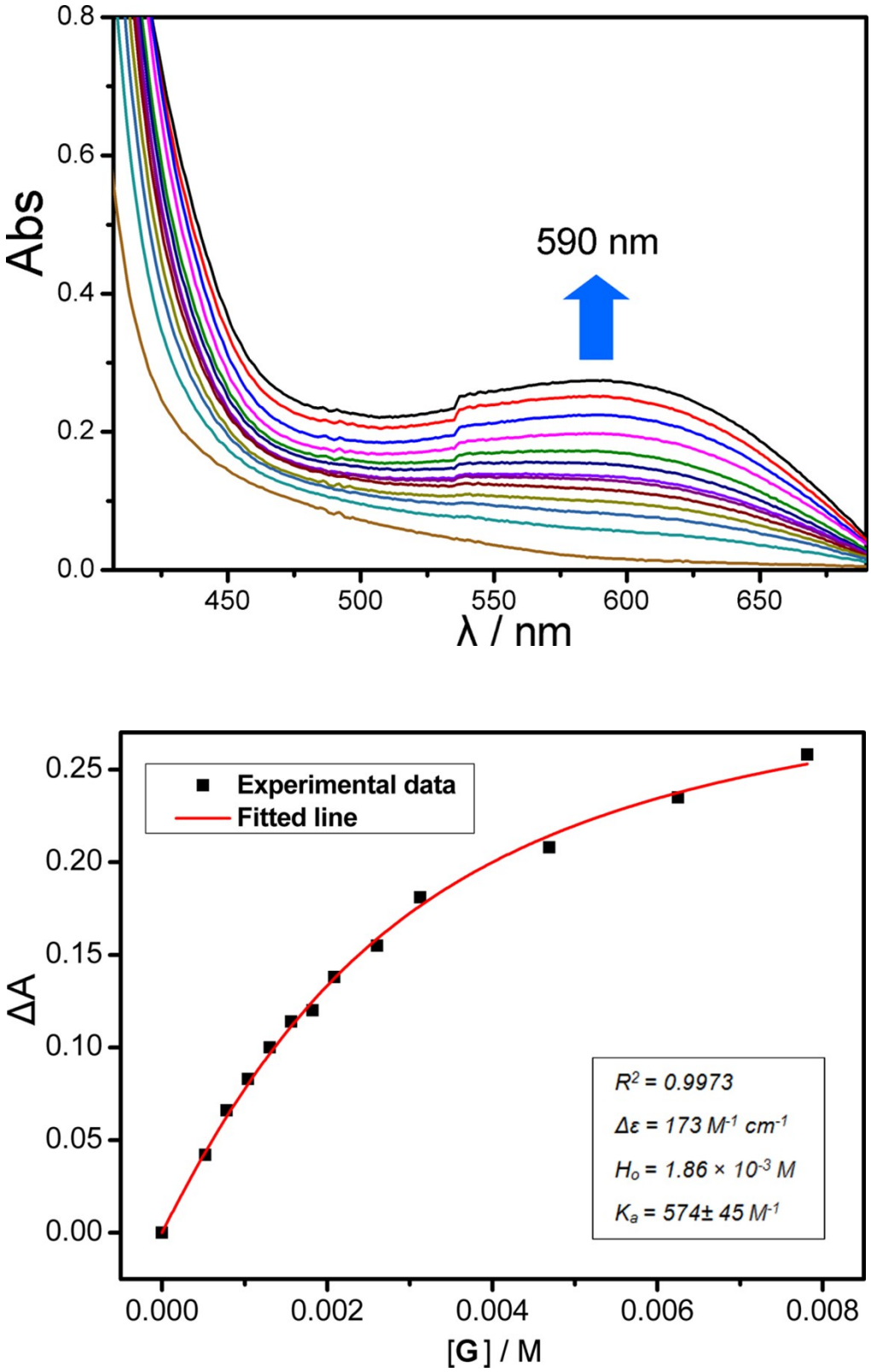

Fig. S35. Top: Stacked UV-Vis spectra obtained by titrating benzidine (**G3**) into a CH_3CN solution of **TBox-1**·$2PF_6$ (1.86×10^{-3} M) at 298 K; Bottom: The nonlinear curve-fitting for the complexation of **TBox-1** with **G3** to give an association constant of 574 ± 45 M^{-1}.

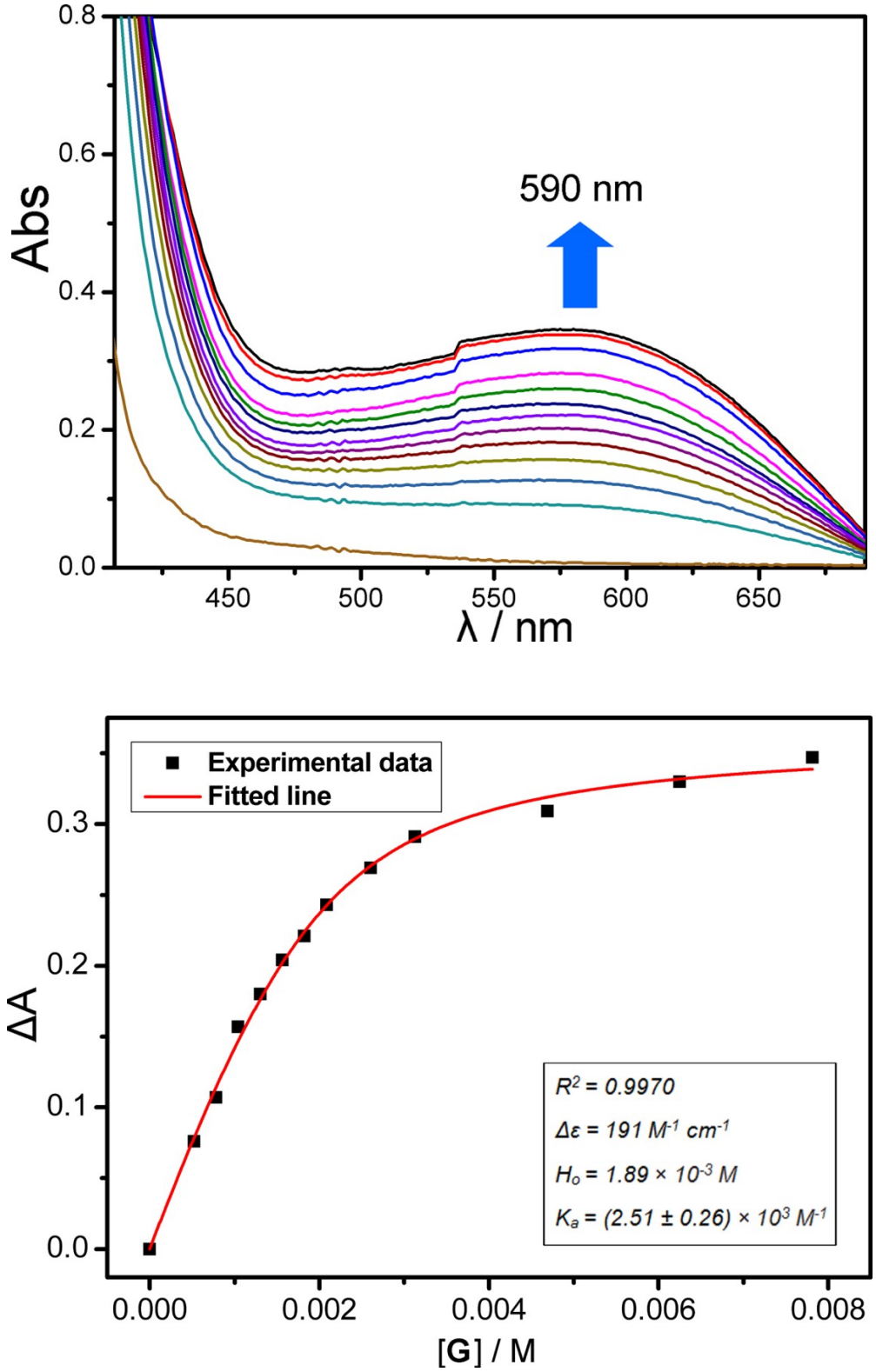

Fig. S36. Top: Stacked UV-Vis spectra obtained by titrating **G3** into a CH_3CN solution of **TBox-2**·$2PF_6$ (1.89×10^{-3} M) at 298 K; Bottom: The nonlinear curve-fitting for the complexation of **TBox-2** with **G3** to give an association constant of $(2.51 \pm 0.26) \times 10^3$ M^{-1}.

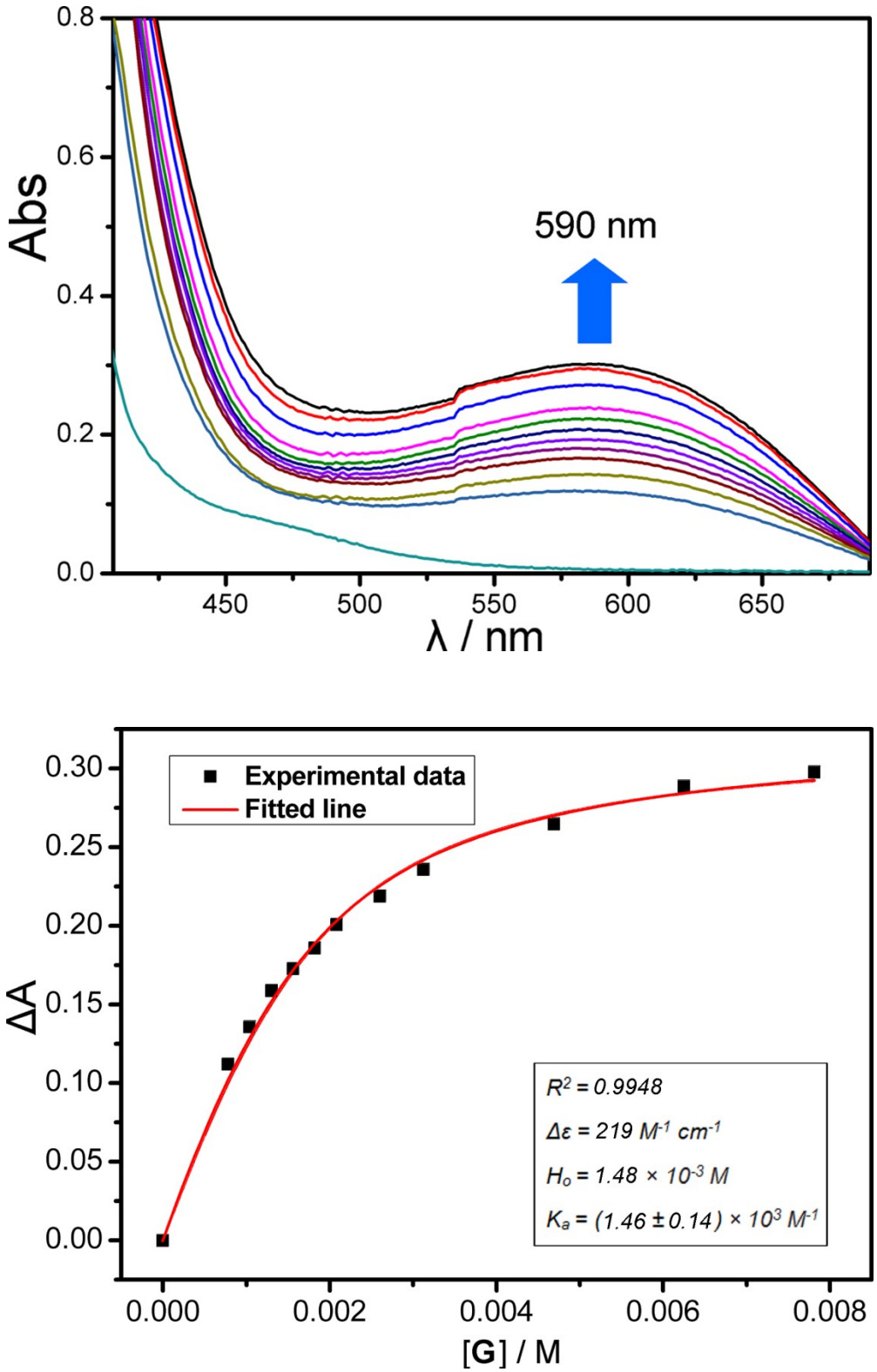

Fig. S37. Top: Stacked UV-Vis spectra obtained by titrating **G3** into a CH_3CN solution of **TBox-3**·$2PF_6$ (1.48×10^{-3} M) at 298 K; Bottom: The nonlinear curve-fitting for the complexation of **TBox-3** with **G3** to give an association constant of $(1.46 \pm 0.14) \times 10^3$ M^{-1}.

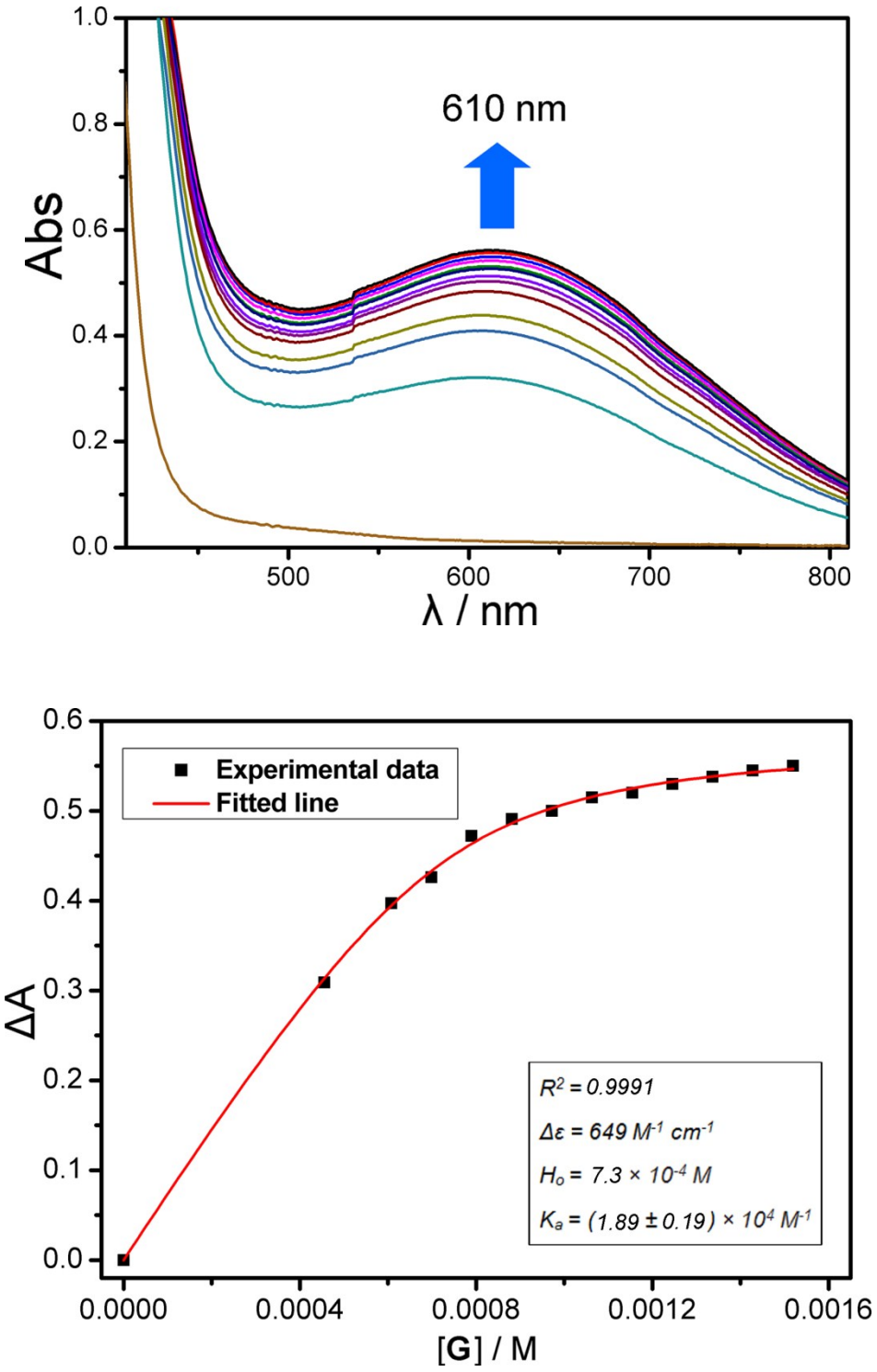

Fig. S38. Top: Stacked UV-Vis spectra obtained by titrating **G3** into a mixed water/methanol solution (9:1, v/v) of **TBox-1**·2Cl (7.3×10^{-4} M) at 298 K. The mixed solution was used because of the low solubility of **G3** in pure water. Bottom: The nonlinear curve-fitting for the complexation of **TBox-1** with **G3** to give an association constant of $(1.89 \pm 0.19) \times 10^4$ M^{-1}.

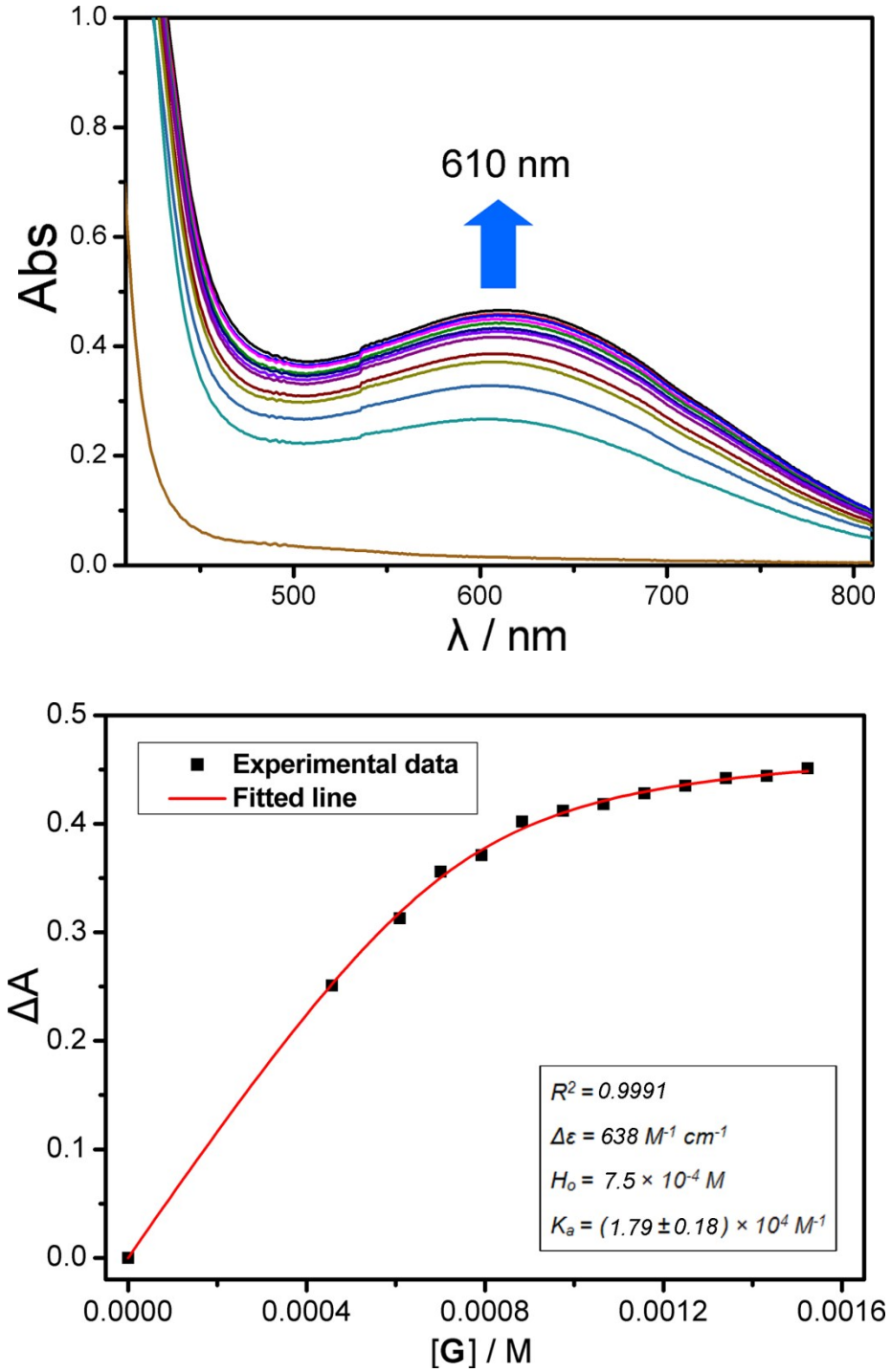

Fig. S39. Top: Stacked UV-Vis spectra obtained by titrating **G3** into a mixed water/methanol solution (9:1, v/v) of **TBox-2**·2Cl (7.5×10^{-4} M) at 298 K. The mixed solution was used because of the low solubility of **G3** in pure water. Bottom: The nonlinear curve-fitting for the complexation of **TBox-2** with **G3** to give an association constant of $(1.79 \pm 0.18) \times 10^4$ M^{-1}.

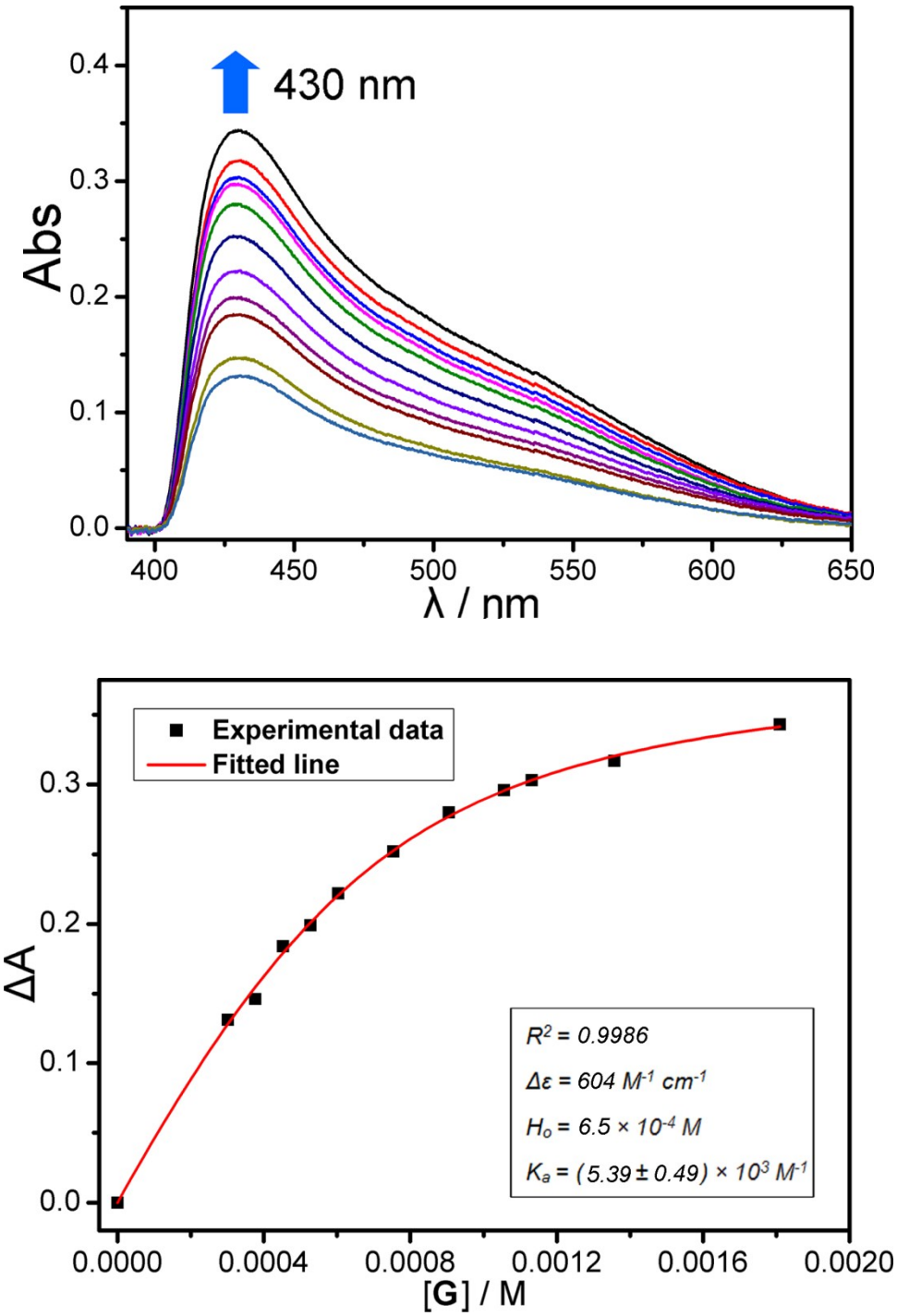

Fig. S40. Top: Stacked UV-Vis spectra obtained by titrating Tryptophan (Trp) into a aqueous solution of **TBox-1**·2Cl (6.5×10^{-4} mol/L) at 298 K. For clarity of absorption bands of host-guest complex at 420 nm, the absorption of host **Tbox-1** has been subtracted. Bottom: The nonlinear curve-fitting for the complexation of **Tbox-1** with Trp to give an association constant of $(5.39 \pm 0.49) \times 10^3$ M^{-1}.

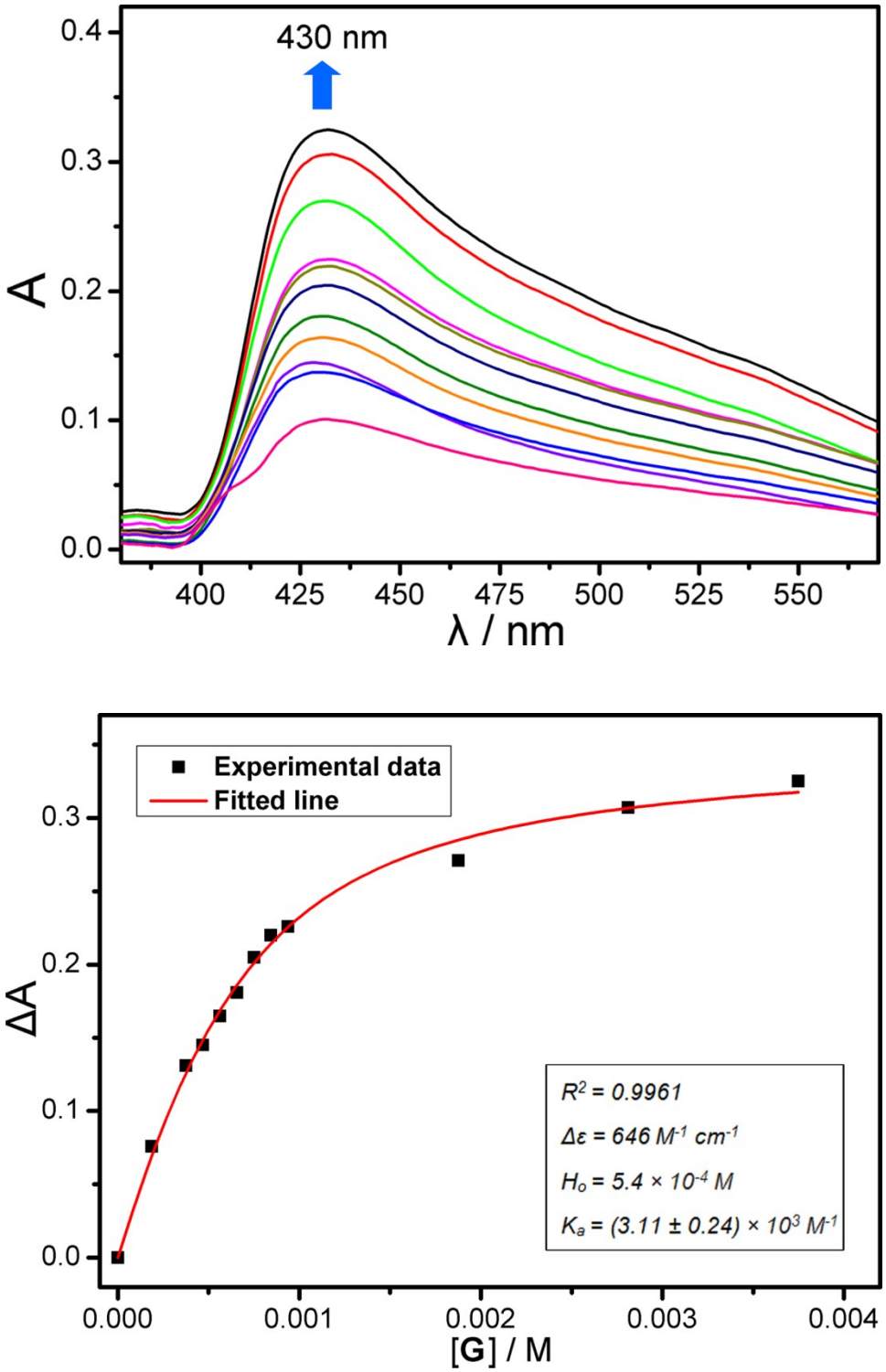

Fig. S41. Top: Stacked UV-Vis spectra obtained by titrating Trp into a 10 mM Tris buffer solution (pH = 7.2) of **TBox-1**·2Cl (5.4×10^{-4} M) at 298 K. For clarity of absorption bands of host-guest complex at 430 nm, the absorption of host **Tbox-1** has been subtracted. Bottom: The nonlinear curve-fitting for the complexation of **Tbox-1** with Trp to give an association constant of $(3.11 \pm 0.24) \times 10^3$ M^{-1}.

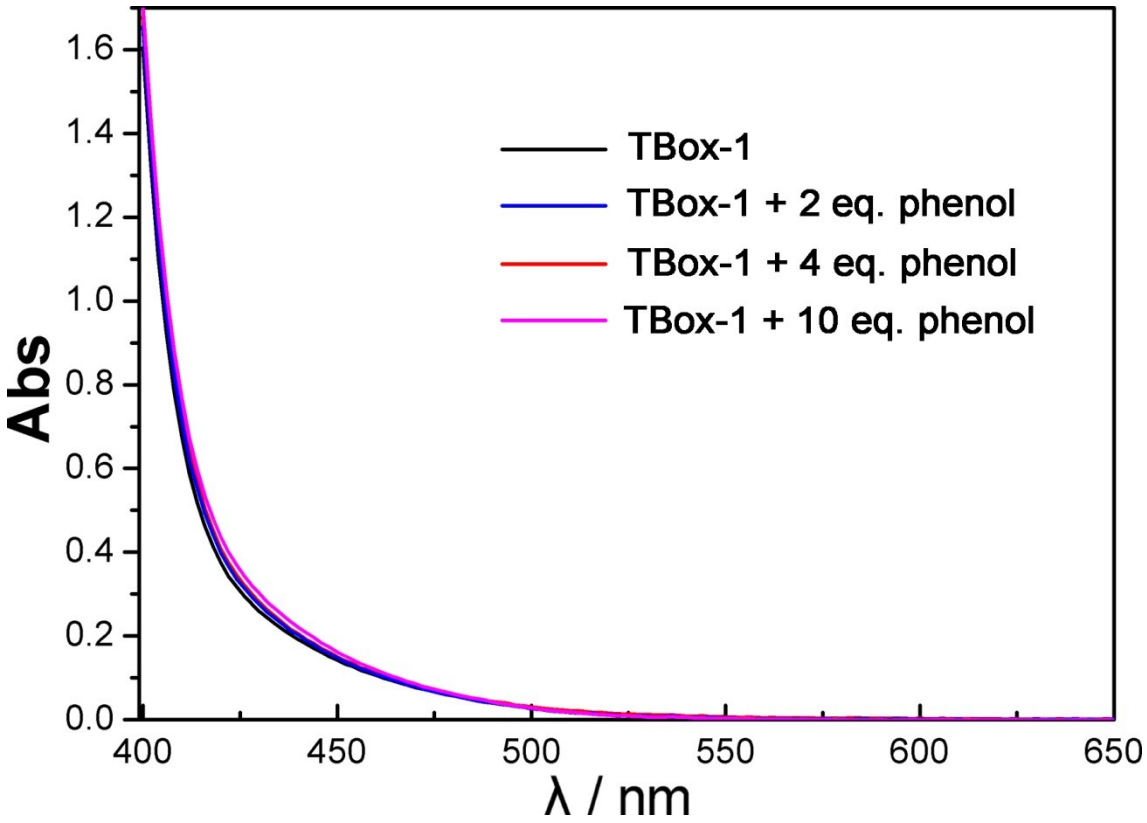

Fig. S42. UV-Vis spectra obtained by adding various amount of phenol into a aqueous solution of **TBox-1**·2Cl (5.8×10^{-3} mol/L) at 298 K. The result shows that the extent of curve change upon mixing phenol and **TBox-1** solution was so small that it failed to determine the association constants by UV-vis titration.

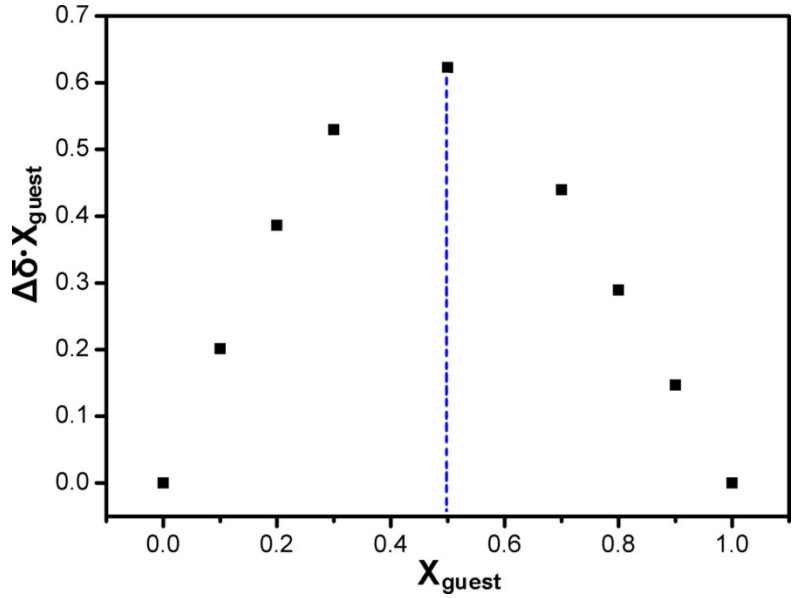

Fig. S43. Job's plot constructed from the Δδ in chemical shift of the guest's indol proton H_4 (for proton designations, see Figure 5) in ^{1}H NMR spectra by varying the ratio between Trp and **TBox-1**·2Cl with a fixed total concentration ([Trp] + [**TBox-1**] = 1.0 mM). This experiment supports the 1:1 binding stoichiometry between Trp with **TBox-1**·2Cl in D_2O.

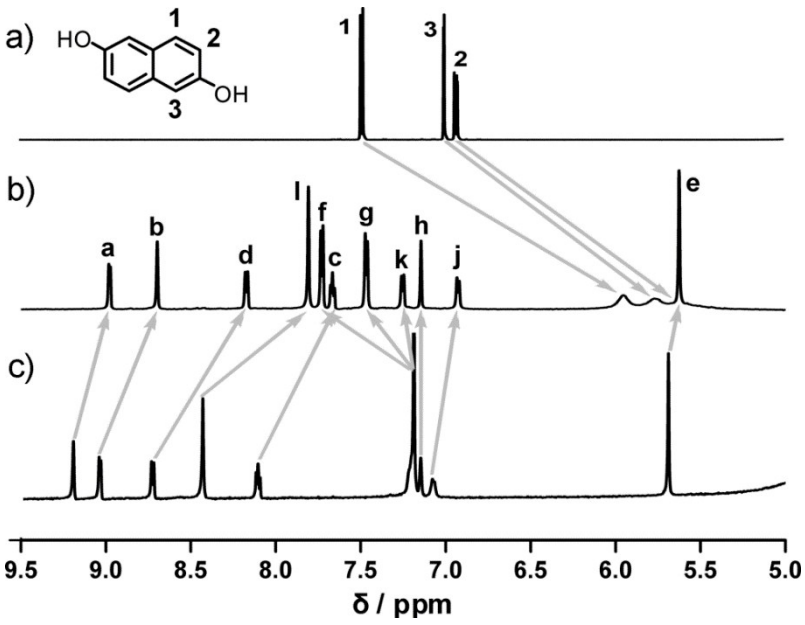

Fig. S44. ^{1}H NMR spectra (600 MHz, D_2O : CD_3OD = 2 : 1, 298 K) of a) **G2**, c) **TBox-1**, and b) their equimolar mixture. These spectra verify the formation of the host-guest complex between **G2** and **TBox-1**.

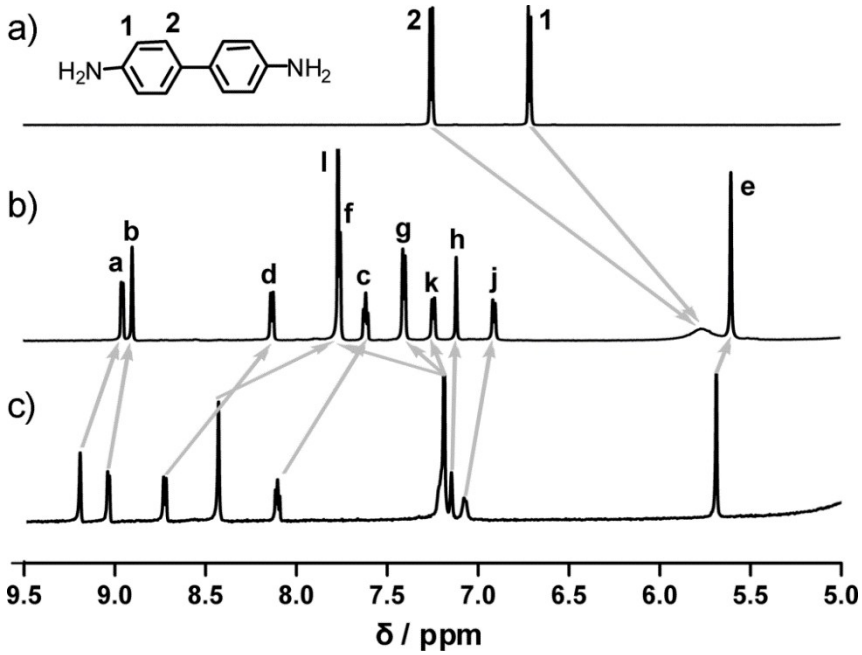

Fig. S45. ^{1}H NMR spectra (600 MHz, D_2O : CD_3OD = 2 : 1, 298 K) of a) **G3**, c) **TBox-1**, and b) their equimolar mixture. These spectra verify the formation of the host-guest complex between **G3** and **TBox-1**.

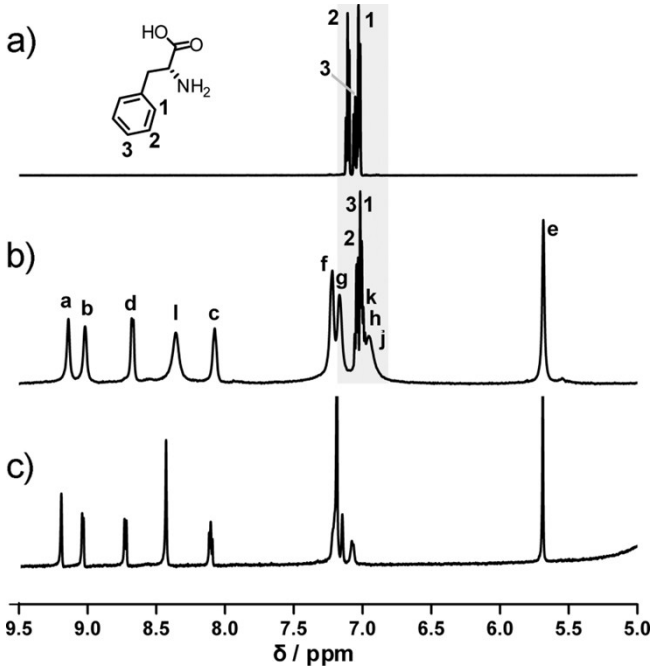

Fig. S46. ^{1}H NMR spectra (600 MHz, D_2O : CD_3OD = 2 : 1, 298 K) of a) phenylalanine, c) **Tbox-1**, and b) their equimolar mixture. These spectra indicate that **Tbox-1** shows very little affinity for phenylalanine.

5. Computational Studies

In the present work, the electronic structural property of **Tbox-1** crystal was investigated by using the DFTB+ free software that is an implementation of the Density Functional based Tight Binding (DFTB) method.[S4] Due to the large deformation of the optimized geometry, calculations for **Tbox-1** were based upon its crystal data, and the default 3ob Slater-Koster atomic parameters and Fine quality were adopted for calculations. For the three amino acid molecules, the geometries were fully optimized in aqueous solution and were confirmed as the energy minima by the absence of imaginary frequency. And then the electronic structural properties were studied at the BLYP-D3BJ/def2-TZVP level of thery.[S5] The COSMO[S6] approach was used to describe the solvation effect, and all of these calculations were performed using the ORCA software.[S7]

Table S2 The electronic structural properties for **Tbox-1** crystal and three amino acids

	Eg(eV)	E_{HOMO} (eV)	E_{LUMO} (eV)
Tbox-1	1.14	-6.02	-4.88
Trp	3.54	-4.82	-1.28
Phe	4.28	-5.68	-1.40
Tyr	3.97	-5.28	-1.31

	HOMO	LUMO
Tbox-1	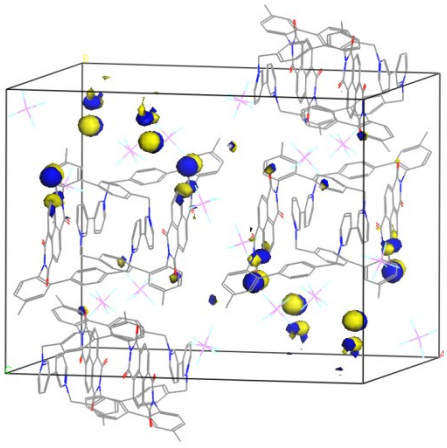	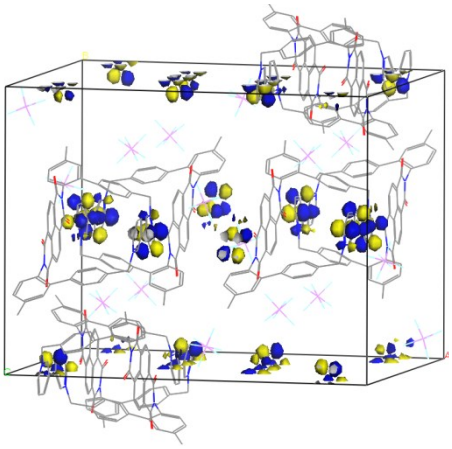
Trp	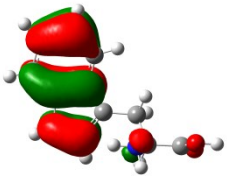	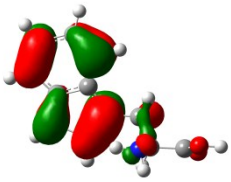
Phe	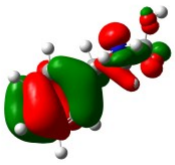	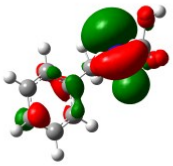
Tyr	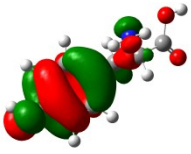	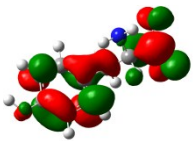

Fig. S47. Plots of the molecular orbitals of the **Tbox-1** crystal and three amino acids. It shows that LUMO of **Tbox-1** is mainly composed of the π-orbitals of bipyridinium, and HOMO of Trp is mainly formed by the π-orbitals of indole moiety. Thus, the molecular orbital plots further conform the presence of π-π charge transfer between the LUMO of **Tbox-1** and HOMO of Trp.

References:

[S1] G. M. Sheldrick, SADABS: Program for Empirical Absorption Correction of Area Detector Data; University of Göttingen, Göttingen, Germany, 1996.

[S2] G. M. Sheldrick, SHELXL-97, Program for Solution of Crystal Structures, University of Göttingen, Göttingen, Germany, 1997.

[S3] H. Cong, L.-L. Tao, Y.-H. Yu, Z. Tao, F. Yang, Y.-J. Zhao, S.-F. Xue, G. A. Lawrance, G. Wei, *J. Phys. Chem. A* 2007, 111, 2715-2721.

[S4] B. Aradi, B. Hourahine, Th. Frauenheim, *J. Phys. Chem. A*, **2007**, 111, 5678.

[S5] a) A. D. Becke, *Phys. Rev. A*, **1988**, 38, 3098; b) C. Lee, W. Yang, and R. G. Parr, Phys. Rev. B, 1988, 37, 785; c) A. Schaefer, H. Horn and R. Ahlrichs, *J. Chem. Phys.***1992**, 97, 2571; d) F. Weigend, R. Ahlrichs, *Phys. Chem. Chem. Phys.***2005**, 7, 3297; f) S.Grimme, S.Ehrlich, L.Goerigk, *J Comput. Chem.* **2011**, 32, 1456; g) S.Grimme, J.Antony, S.Ehrlich and H.Krieg, *J.Chem.Phys.* **2010**, 132, 154104.

[S6] A. Klamt, G. Schüürmann, *J. Chem. Soc. Perkin Trans.* **1993**, 2, 799.

[S7] F. Neese, The ORCA program system, Wiley Interdiscip. Rev.: Comput. Mol. Sci. **2012**, 2, 73-78.